

ULTRAHIGH VACUUM ELECTROCHEMICAL STUDIES OF METALS AND
SEMICONDUCTOR DEPOSITION

by

DANIEL KEBREAB GEBREGZIABIHER

(Under the Direction of John Lewellen Stickney)

ABSTRACT

This dissertation describes the growth of nano films by electrochemical methods in an ultrahigh vacuum system (UHV) that is compatible with electrochemical deposition process. The UHV system was equipped with surface analysis techniques such as Auger electron spectroscopy (AES), low energy electron diffraction optics (LEED) and X-ray photoelectron spectroscopy (XPS). The first part of this dissertation deals with the electrodeposition of copper (Cu) nanofilms as seed layers on ruthenium (Ru) barrier layer for the metallization of integrated circuits. The Cu nano film was deposited by using lead (Pb) as a sacrificial element. A Pb UPD was deposited and this UPD was exchanged for Cu by flowing a solution of Cu^{+2} ions at open circuit potential in a redox replacement reaction. Since Cu is more noble than Pb, the Cu ions take electrons from Pb to be deposited as Cu atoms. The process should ideally result in the formation of only an atomic layer of Cu. This constituted one deposition cycle and the cycle was repeated several times to grow the Cu nano film. As a continuation of this study, Cu surface passivation was investigated by depositing atomic layers (AL) of different elements on Cu(111). The elements investigated for the passivation of Cu from oxidation included

selenium (Se), iodine (I) and tellurium (Te). The purpose of this study was to protect Cu surface from contamination between solutions in a Fab line. The Se, I and Te modified Cu(111) was exposed to ambient air, solution vapors and oxygen and it was concluded that an atomic layer of Te protects the Cu(111) surface the best out of the investigated elements.

The second part of this dissertation deals with electrodeposition of germanium (Ge), a semiconductor, from an aqueous solution of Ge. The composition of the deposits was studied using AES and the surfaces were characterized using STM. Analytical techniques such as cyclic voltammetry (CV) and electrochemical quartz microbalance (EQCM) were used to follow the electrodeposition process. It was concluded that the electrochemical deposition of Ge from an aqueous solution was self-limiting even though bulk deposition potentials were used. At very negative potentials Ge forms a germanium hydride passivating layer.

INDEX WORDS: Copper, Germanium, UHV, AES, UPD, LEED, STM, EQCM, CV, Electrodeposition, Redox Replacement Reactions, Mono-layer, Sacrificial element.

ULTRAHIGH VACUUM ELECTROCHEMICAL STUDIES OF METALS AND
SEMICONDUCTOR DEPOSITION

by

DANIEL KEBREAB GEBREGZIABIHER

BS, Asmara University, Eritrea, 1985

A Dissertation Submitted to the Graduate Faculty of The University of Georgia in Partial
Fulfillment of the Requirements for the Degree

DOCTOR OF PHILOSOPHY

ATHENS, GEORGIA

2012

© 2012

Daniel Kebreab Gebregziabier

All Rights Reserved

ULTRAHIGH VACUUM ELECTROCHEMICAL STUDIES OF METALS AND
SEMICONDUCTOR DEPOSITION

by

DANIEL KEBREAB GEBREGZIABIHER

Major Professor: John L. Stickney
Committee: Jonathan I. Amster
Tina Salguero

Electronic Version Approved:

Maureen Grasso
Dean of the Graduate School
The University of Georgia
December 2012

DEDICATION

To my family, with love.

ACKNOWLEDGEMENTS

I would like to acknowledge Prof. John L. Stickney for keeping me in line and making me think like a scientist. Without his guidance and support I would not be where I am now. I would also like to acknowledge my committee members Prof. Jonathan Amster and Prof. Tina Salguero for their advice and guidance. I could not ask for a better working environment because my colleagues were the best, present and past. Dr. Jay Kim, Dr. Chandru Thambidurai, Dr. Xuehai Liang, Dr. Nagarajan Jayaraju, Dr. Dego Banga, Leah, Brian, Maria, Chu, Justin, David, Vicky and Kuashik.

My family and friends loved and supported me every inch of the way and I would like to thank them. You have been wonderful and I love you. I would, especially, like to thank my sister Genet and her husband Dr. Tesfay for believing in me and supporting me.

TABLE OF CONTENTS

	Page
ACKNOWLEDGEMENTS	v
LIST OF TABLES	vii
CHAPTER	
1 INTRODUCTION AND LITERATURE REVIEW	1
2 ELECTROCHEMICAL ATOMIC LAYER DEPOSITION OF COPPER NANO FILMS ON RUTHENIUM	23
3 Cu(111) SURFACE PASSIVATION WITH ATOMIC LAYERS OF Te, Se OR I, STUDIED USING AUGER SPECTRSCOPY	50
4 ELECTROCHEMICAL ULTRA HIGH VACUUM STUDIES OF GERMANIUM ATOMIC LAYER FORMATION ON Au(111)	78
5 CONCLUSION.....	97

LIST OF TABLES

	Page
Table 3.1: COMPARISON OF AES PEAK TO PEAK O/CU RATIOS OF MODIFIED CU(111) SURFACE BEFORE EXPOSURE AND AFTER EXPOSURE TO SOLUTION VAPORS AND AMBIENT AIR	62

CHAPTER 1

INTRODUCTION AND LITERATURE REVIEW

The main focus of this dissertation is electrochemical atomic layer deposition (EC-ALD) of Cu on 10 nm e-beam sputtered Ru on silicon and EC-ALD of Ge on Au(111) single crystal from aqueous solutions. Chapter 2 introduces Cu nano-film formation on Ru by EC-ALD. In this study the growth of Cu films on 10 nm of e-beam sputtered Ru on Si was performed using EC-ALD [1-3] [4-8]. ALD is the layer by layer formation of nano-films, using surface limited reactions in a cycle [9-13]. Underpotential deposition (UPD) is a name for an electrochemical surface limited reaction, a phenomenon where an atomic layer of one element can form on a second element at a potential prior to or under that needed to deposit the element on itself [14-19]. This results from the free energy of formation of a surface compound or alloy.

The deposition of Cu films in this study started with direct UPD of Cu on the 10nm Ru nano-film on Si as the first cycle in the Cu EC-ALD. A second atomic layer of Cu could not be formed by the same method given the definition UPD above. In order to form the second and subsequent atomic layers of Cu, monolayer galvanic displacement [20, 21], also referred to as surface limited redox replacement [8, 22-26] was used. Since UPD Cu cannot be formed on Cu, an atomic layer of a less noble element was first formed via UPD (the sacrificial layer). Next, a solution containing Cu^{2+} ions was introduced at open circuit potential (OCP) and allowed to exchange by redox replacement for the sacrificial element. The limited nature of this process comes from the amount of

the sacrificial element deposited which can only deliver a finite number of electrons. According to Faraday's 1st law of electrolysis that number of electrons stipulates the maximum amount of Cu that can be formed in a cycle.

In the present study, Pb UPD was used to form the sacrificial layers. The Pb²⁺ solution was then replaced with a Cu²⁺ solution at OCP, facilitating exchange of Pb for Cu. This constituted one ALD cycle and was repeated up to seven times in these studies. Figure 1.1 shows the cartoon of this process. This concept of surface limited redox replacement was inspired by the work of Adzic, Brankovic, and Wang [27] who were using "monolayer galvanic replacement" to form fractions of a monolayer of Pt in studies of fuel cell catalyst reactions. Mike Weaver et al. repeated this process up to 8 cycles in what appears to be the first example of EC-ALD of a pure element [21]. The process of surface limited redox replacement has been described in more depth elsewhere [28-30].

The present investigation made use of an ultra-high vacuum (UHV) surface analytical instrument, equipped with AES and LEED, in combination with electrochemical experiments performed within a UHV compatible ante-chamber in a process referred to as UHV-EC [31, 32]. Figure 1.2 shows the picture of the UHV-EC system that was used for these studies. The main and ante chambers were maintained at UHV by a combination of ion and cryo-pumps. Prior to any electrochemical studies, the working electrode was cleaned by Ar⁺ ion bombardment inside the ion bombardment cage (Figure 1.2B) by leaking Ar gas ($\sim 10^{-5}$ torr) into the main chamber. The surface of the working electrode roughens after bombardment with Ar⁺ ions and could be smoothed by resistive heating. In addition to smoothing the rough surface, the resistive heating was also useful in getting rid of the impinging primary ions which tend to implant themselves

in the electrode. Hot ion bombardment could also be performed in which the electrode was cleaned and annealed at the same time. The electrode could be transferred through a 4.5" gate valve to the ante-chamber and then isolated from the main chamber and back filled with ultrapure Ar gas to bring it to atmospheric pressure for electrochemical studies. The solutions were being continuously purged with Ar gas for at least 30 minutes before the electrochemical process to remove any dissolved oxygen. The electrochemical studies were performed in a three electrode configuration electrochemical cell and the potentials were controlled by an Autolab potentiostat. After the electrochemical studies the electrochemical cell was withdrawn from the ante-chamber and the ante-chamber was pumped down to UHV. The electrode was then transferred back to the main chamber for characterization.

AES and LEED were used for studying the composition and the orientation of the deposits respectively. AES is a three electron process in which primary high energy electrons (~ 3 KeV) are used to eject a core electron creating a hole. Since this is an unstable state a valence electron drops down to fill the hole by releasing energy which is enough to eject another valence electron into vacuum, the Auger electron [33]. Figure 1.3 shows the schematics of a KL_2L_3 Auger process. The ejected Auger electron is then deflected to a cylindrical mirror analyzer (CMA) multiplied by passing it through an electron multiplier and detected. Auger electrons have kinetic energies which are characteristic to an element and are functions of the binding energies of the electrons. The kinetic energy of the Auger electron can be described by: $E_{K.E} = E_K - E_{L_2} - E_{L_3}$, where E_K , E_{L_2} , and E_{L_3} are the binding energies. The collected Auger electrons were plotted as a function of energy against a broad secondary electron background spectrum

and therefore AES was run in the derivative mode to enhance the signals. Figure 1.4 is an example of a Ru AES after it has been cleaned by Ar⁺ ion bombardment. Since AES is a three electron process hydrogen and helium cannot be detected by using AES.

LEED is a surface analytical technique which can be used for the determination of surface structures. It can be used qualitatively to obtain information on the size, symmetry and rotational alignment of the adsorbate unit cell with respect to the substrate unit cell [34]. Low energy electrons in the range of 20 -200 eV are emitted from a filament which is held at a negative potential and these electrons are focused by electrostatic lenses and are then accelerated towards the grounded sample. The impinging primary electrons on the sample are then backscattered either elastically or inelastically off the sample surface [35]. Figure 1.5 shows a LEED display set up. The backscattered electrons are accelerated towards grid 1 which is kept at ground and a retardation potential is applied to grid 2 to allow only the elastically scattered electrons to accelerate towards grid 3 which is kept at ground. Finally the elastically scattered electrons accelerate towards the phosphor screen which is held at a positive potential of 5 KV. The elastically backscattered electrons form a pattern when they hit the phosphor screen if the surface of the sample is ordered.

The Damascene process for deposition of Cu interconnects must scale down according to Moore's law [36]. Damascene Cu deposition for the Back End of ultra-large system integration (ULSI) requires a liner to prevent inter-diffusion of Cu into the Si/SiO₂ and to facilitate Cu electrodeposition [37-39]. Presently, Ta/TaN diffusion barriers are used to isolate Cu from the dielectric material. Direct electrodeposition of Cu on such barrier layers is difficult due to high electrical resistance of the barrier layers so a

seed layer of Cu, formed by physical vapor deposition (PVD), is generally inserted between the barrier layers and the Damascene Cu [37-39] to complete the liner. However, obtaining a conformal Cu seed layer by PVD can be difficult in very low dimensions or high aspect ratios, resulting in problems such as uneven filling of trenches and vias and defects in the deposit. The use of Cu in the Back End was adopted to enhance IC performance by reducing RC delay times [40]. However, as the feature size decreased, and aspect ratios increased, new challenges were created to the deposition of conformal liners [37].

Ruthenium has lower thermal and electrical resistivity when compared to Ta/TaN and its low solubility in copper makes it a candidate for Cu metallization barrier layers. Perng et al. reported that ultra-thin ruthenium is stable as a barrier layer up to 300⁰C and suggested that doping the ruthenium with phosphorus may help its barrier properties at higher temperatures, even though the sheet resistance increases slightly [40]. Another advantage of ruthenium as a barrier layer is that it has strong adhesion to Cu, which can then be directly plated. Chan et al reported that a 20 nm ruthenium barrier layer can prevent copper diffusion up to a temperature of 450⁰C [41] and Arunagiri et al. demonstrated that 5nm ruthenium can act as a platable Cu diffusion barrier up to 300⁰C [42]. According to Wei et al. Cu starts to diffuse through 1nm ruthenium around 300⁰C [43]. Soo et al. reported that ALD-Ru (4nm)/ALD-TaCN (2nm) prevented copper diffusion up to 550⁰C and increasing the ALD-Ru to 12nm prevented the diffusion of copper up to a temperature of 600⁰C for 30 minutes [44].

Moffat et al. claim that the presence of an oxide results in weak Cu-Ru adhesion and may even prevent copper under potential deposition (UPD) [37, 45]. They also claim

that the deposition of copper occurs competitively with oxide reduction, which may control its deposition kinetics. They suggest that the 3-D oxide can be reduced by polarizing the ruthenium near the hydrogen evolution region [37] prior to exposure to the Cu solution.

It was demonstrated by Stickney et al that adsorbing I atoms on some metal surfaces can prevent surface contamination and oxidation under ambient conditions [46]. Kelber et al. reported that adsorbing I atoms from I₂ at 300K passivated a ruthenium surface against oxidation. In addition, during overpotential Cu electrodeposition (OPD), the I atoms floated on top of the depositing Cu, thus maintaining the protection as the deposit grew [47]. The Stickney group has also studied the adsorption of Cl on Cu single crystal surfaces, where it was also shown to protect the surface, while forming a well ordered atomic layer [48-50].

In Chapter 3 the passivation of copper by the adsorption of single atomic layers (AL) of elemental surfactants is discussed. Electrochemical deposition of selenium, tellurium or iodine atomic layer on Cu(111) surfaces were studied using cyclic voltammetry to investigate the potential dependence, AES to follow surface composition, and LEED to indicate surface order.

Copper is one of the most important elements in microelectronics and is used on the back end of ULSI as the on-chip wiring material [51-55]. Due to its lower electrical resistance and susceptibility to electro-migration, copper replaced aluminum in integrated circuits as the interconnect material of choice [38, 56]. The electrochemical process for Cu on chip wiring is referred to as the Damascene process and its ability to achieve

bottom up filling of vias and high aspect ratio trenches is particularly important to present ULSI designs [38, 55].

Copper is a relatively active metal and readily oxidizes in ambient air, forming a mixture of oxides and hydroxides (i.e. Cu_2O , CuO and $\text{Cu}(\text{OH})_2$) which can build up tensile stress [56]. The oxide layer can result in poor electrical conductivity of the copper and can cause material degradation. It is therefore of interest to minimize the oxidation of copper between steps on the fab floor. Oxidation can easily be avoided if the wafer is in solution and under potential control. However when the wafer is moved from one plating bath to the next it can lose potential control (go open circuit) and oxidize to some extent in the aqueous electrolyte plating solutions, unless the surface is protected from oxidation during transfer.

Adsorption of halides on metal surfaces has been extensively studied over the years [47, 57-60]. UHV-EC studies by Kim J.Y. et al. [44] have shown that an adsorbed layer of chloride protects copper after emersion (withdrawal) from solution, before pumping to UHV and transferring to the analysis chamber for surface characterization. Iodine adsorbed on metal surfaces can also protect the surfaces from contamination while at the same time acting as a surfactant which allows electrodeposition to proceed [47, 61].

Chapter 4 describes the electrochemical deposition of Ge on Au(111) single crystal. The purpose of this study was to investigate electrodeposition of germanium on Au(111) single crystal from aqueous solutions and study the interaction between the first layer of germanium and the gold single crystal. If the first atomic layer can be deposited and its growth controlled, then this phenomena can be used for growing atomic layers of germanium which can be used for optoelectronic materials.

The success of Si for electronic applications was due to its almost perfect interface with its thermally grown oxide which acts as an effective mask in device manufacturing and an extremely low surface state density at the Si/SiO₂ interface [62]. But further scaling down of Si/SiO₂ based transistors is at an end for future high performance devices.

Germanium is of interest because it has high hole and electron mobility as compared to silicon [63, 64]. In Si based devices, germanium has possible applications as a photo-detector and high mobility channel field effect transistors and it can also be used as a substrate for growing III-V compound semiconductors in multi-junction photovoltaic cells [65, 66]. Some of the limitations of germanium are that it is expensive [67], has higher density of states and a narrower band gap when compared to silicon and its thermally grown oxide is not as perfect and as good a dielectric as silicon dioxide [62]. The deposition of high-*k* dielectric materials such as HfO₂, Al₂O₃, and ZrO₂ on germanium substrate have been reported [68] and these materials could improve to alleviate the not so perfect GeO₂.

The electrochemical deposition of germanium has mainly been achieved from ionic solutions due to high hydrogen evolution rate (low hydrogen over-potential) in aqueous solutions [69, 70]. Epitaxial growth of germanium by molecular beam epitaxy (MBE) and ultrahigh vacuum chemical vapor deposition (UHV-CVD) [65] have been reported.

Conclusion of the work and future studies are discussed in Chapter 5.

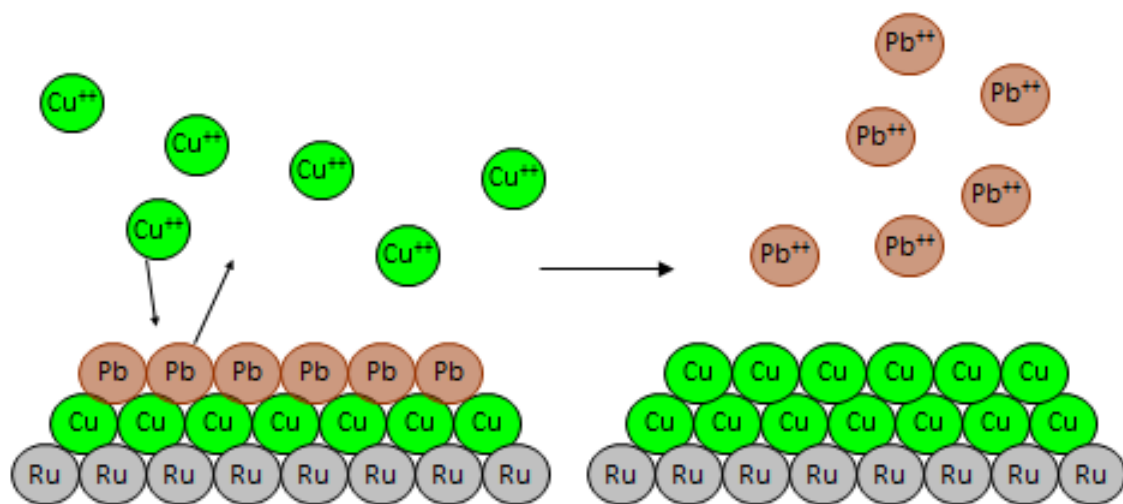
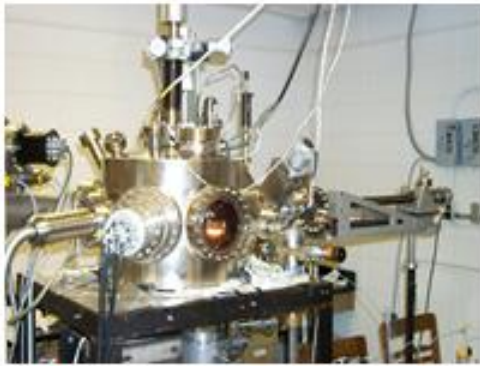


Figure 1.1. A cartoon of surface limited redox replacement reaction of Pb with Cu, in which UPD Pb is replaced by Cu at open circuit potential.



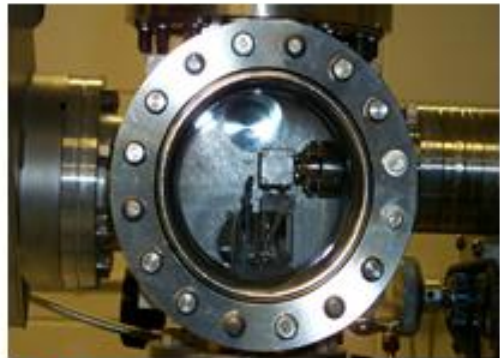
A



B



C



D

Figure 1.2. (A) UHV-EC system, (B) Ion bombardment cage, (C) Reverse view LEED optics and (D) Ante-chamber with electrochemical cell and three electrode configuration.

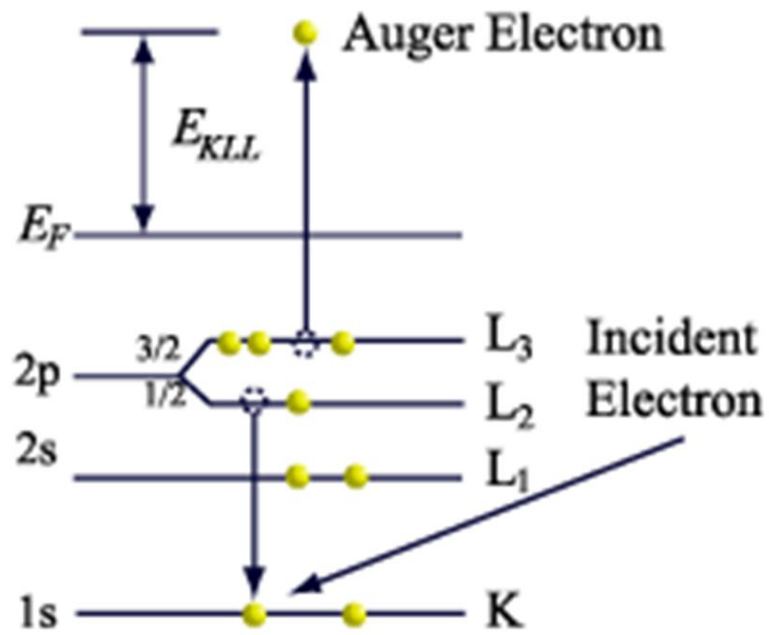


Figure 1.3. Auger KL_2L_3 transition (J. C. Vickerman, *Surface analysis – the principal techniques*, John Wiley & Sons, 1997)

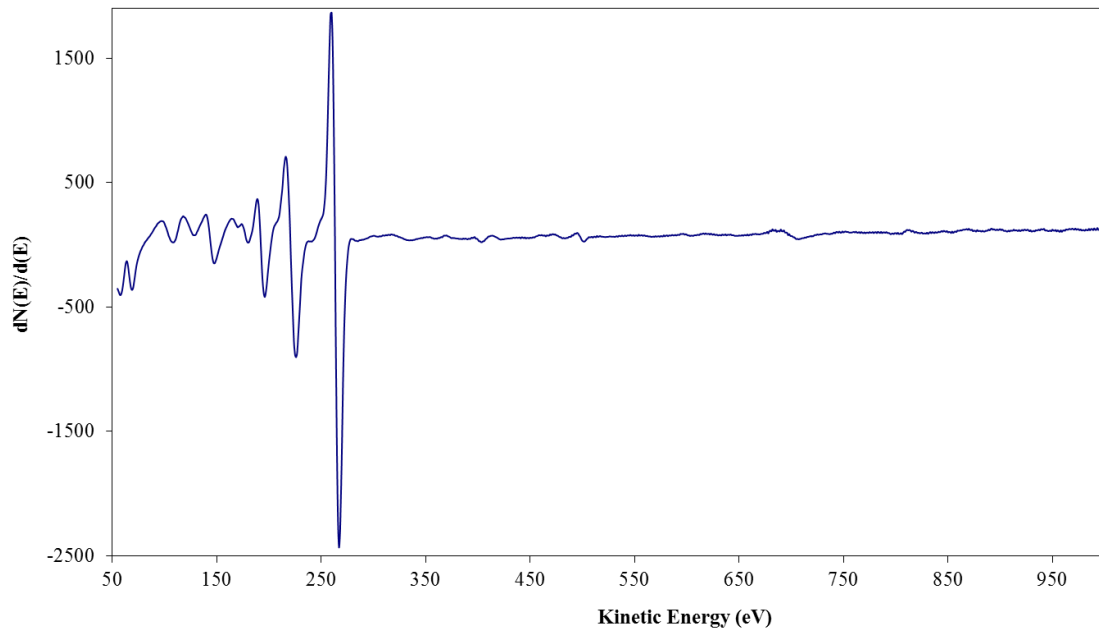


Figure 1.4. AES spectra of a clean cold ion bombarded 10 nm Ru nano-film on Si.

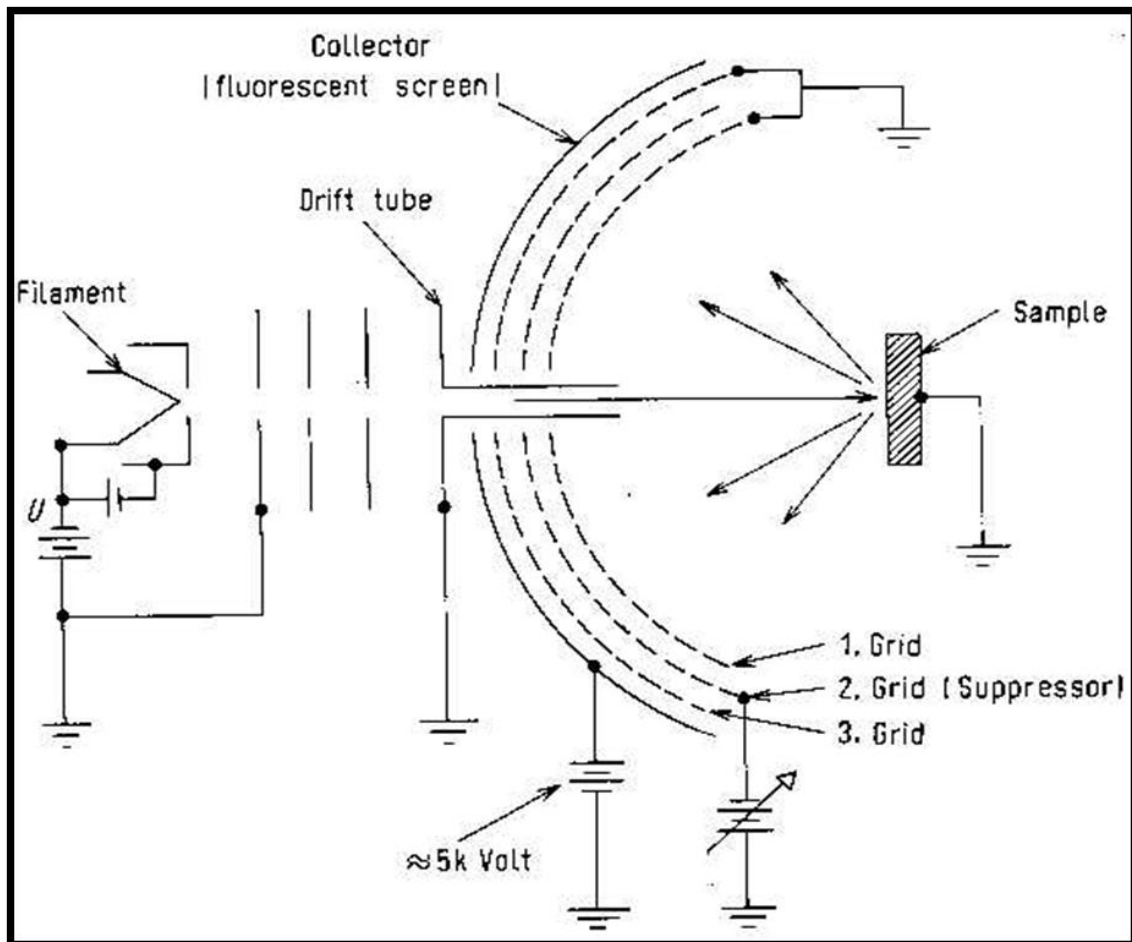


Figure 1.5. Schematic of LEED display set up (Ranke, Surface Analysis, Dept. AC, Fritz Haber Institute of the MPG, Berlin, Germany).

References

1. Gregory, B.W., D.W. Suggs, and J.L. Stickney, *Conditions for the deposition of cadmium telluride (CdTe) by electrochemical atomic layer epitaxy*. Journal of the Electrochemical Society, 1991. **138**(5): p. 1279-84.
2. Colletti, L.P., B.H. Flowers, and J.L. Stickney, *Formation of Thin-Films of CdTe, CdSe, and CdS by Electrochemical ALE*. JECS, 1997.
3. Foresti, M.L., et al., *Electrochemical atomic layer epitaxy deposition of CdS on Ag (111): An electrochemical and STM investigation*. Journal of Physical Chemistry B, 1998. **102**(38): p. 7413-7420.
4. Villegas, I. and P. Napolitano, *Development of a continuous-flow system for the growth of compound semiconductor thin films via electrochemical atomic layer epitaxy*. Journal of the Electrochemical Society, 1999. **146**(1): p. 117.
5. Pezzatini, G., et al., *Formation of ZnSe on Ag(111) by electrochemical atomic layer epitaxy*. Journal of Electroanalytical Chemistry, 1999. **475**(2): p. 164-170.
6. Zou, S. and M.J. Weaver, *Surface-enhanced Raman spectroscopy of cadmium sulfide/cadmium selenide superlattices formed on gold by electrochemical atomic-layer epitaxy*. Chemical Physics Letters, 1999. **312**(2-4): p. 101-107.
7. Torimoto, T., et al., *Preparation of size-quantized ZnS thin films using electrochemical atomic layer epitaxy and their photoelectrochemical properties*. Langmuir, 2000. **16**(13): p. 5820-5824.
8. Kim, Y.G., et al., *Platinum nanofilm formation by EC-ALE via redox replacement of UPD copper: Studies using in-situ scanning tunneling microscopy*. Journal of Physical Chemistry B, 2006. **110**(36): p. 17998-18006.

9. George, S.M., J.D. Ferguson, and J.W. Klaus, *Atomic layer deposition of thin films using sequential surface reactions*. Materials Research Society Symposium Proceedings, 2000. **616**(New Methods, Mechanisms and Models of Vapor Deposition): p. 93-101.
10. Ritala, M. and M. Leskela, *Atomic layer deposition*. Handbook of Thin Film Materials, 2002. **1**: p. 103-159.
11. Gordon, R.G., *Review of recent progress in atomic layer deposition (ALD) of materials for micro- and nano-electronics*. PMSE Preprints, 2004. **90**: p. 726-728.
12. Ritala, M., *Atomic layer deposition*. High-k Gate Dielectrics, 2004: p. 17-64.
13. Shen, C., X.-y. Liu, and G.-z. Huang, *Atomic layer deposition and its applications in semiconductor*. Zhenkong, 2006. **43**(4): p. 1-6.
14. Kolb, D.M., *Physical and Electrochemical Properties of Metal Monolayers on Metallic Substrates*, in *Advances in Electrochemistry and Electrochemical Engineering*, H. Gerischer and C.W. Tobias, Editors. 1978, John Wiley: New York. p. 125.
15. Juttner, K. and W.J. Lorenz, *Underpotential Metal Deposition on Single Crystal Surfaces*. Z. Phys. Chem. N. F., 1980. **122**: p. 163.
16. Adzic, R.R., *Electrocatalytic Properties of the Surfaces Modified by Foreign Metal Ad Atoms*, in *Advances in Electrochemistry and Electrochemical Engineering*, H. Gerischer and C.W. Tobias, Editors. 1984, Wiley-Interscience: New York. p. 159.
17. Gewirth, A.A. and B.K. Niece, *Electrochemical applications of in situ scanning probe microscopy*. Chem. Rev., 1997. **97**: p. 1129-1162.

18. Herrero, E., L.J. Buller, and H.D. Abruna, *Underpotential Deposition at Single Crystal Electrodes Surfaces of Au, Pt, Ag and other Materials*. Chemical Reviews, 2001. **101**: p. 1897-1930.
19. Magnussen, O.M., *Ordered anion adlayers on metal electrode surfaces*. Chemical Reviews, 2002. **102**(3): p. 679-725.
20. Brankovic, S.R., J.X. Wang, and R.R. Adzic, *Metal monolayer deposition by replacement of metal adlayers on electrode surfaces*. SS, 2001. **474**: p. L173-L179.
21. Mrozek, M.F., Y. Xie, and M.J. Weaver, *Surface-enhanced Raman scattering on uniform platinum-group overlayers: Preparation by redox replacement of underpotential-deposited metals on gold*. Analytical Chemistry, 2001. **73**(24): p. 5953-5960.
22. Thambidurai, C., Y.-G. Kim, and J.L. Stickney, *Electrodeposition of Ru by atomic layer deposition (ALD)*. Electrochimica Acta, 2008. **53**(21): p. 6157-6164.
23. Kim, J.Y., Y.G. Kim, and J.L. Stickney, *Copper nanofilm formation by electrochemical atomic layer deposition - Ultrahigh-vacuum electrochemical and in situ STM studies*. Journal of the Electrochemical Society, 2007. **154**(4): p. D260-D266.
24. Kim, J.Y., Y.-G. Kim, and J.L. Stickney, *Studies of Cu Atomic Layer Replacement, formed by Underpotential deposits, to Form Pt Nanofilms Using Electrochemical Atomic Layer Epitaxy (EC-ALE)*. ECS Transactions, 2006. **1**(30): p. 41-48.

25. Dimitrov, N., R. Vasilic, and N. Vasiljevic, *A Kinetic Model for Redox Replacement of UPD Layers*. *Electrochemical and Solid-State Letters*, 2007. **10**(7): p. D79-D83.
26. Vasilic, R., L.T. Viyannalage, and N. Dimitrov, *Epitaxial growth of Ag on Au(111) by galvanic displacement of Pb and Tl monolayers*. *Journal of the Electrochemical Society*, 2006. **153**(9): p. C648-C655.
27. Brankovic, S.R., J.X. Wang, and R.R. Adzic, *New methods of controlled monolayer-to-multilayer deposition of Pt for designing electrocatalysts at an atomic level*. *Journal of the Serbian Chemical Society*, 2001. **66**(11-12): p. 887-898.
28. Jeong, S.W., et al., *Effects of annealing temperature on the characteristics of ALD-deposited HfO₂ in MIM capacitors*. *Thin Solid Films*, 2006. **515**(2): p. 526-530.
29. Vasilic, R. and N. Dimitrov, *Epitaxial Growth by Monolayer-Restricted Galvanic Displacement*. *Electrochemical and Solid-State Letters*, 2005. **8**(11): p. C173-C176.
30. Brankovic, S.R., J. McBreen, and R.R. Adzic, *Spontaneous deposition of Pt on the Ru(0001) surface*. *Journal of Electroanalytical Chemistry*, 2001. **503**(1-2): p. 99-104.
31. Hubbard, A.T., *Accounts of Chemical Research*, 1980. **13**: p. 177.
32. Soriaga, M.P. and J.L. Stickney, *Vacuum surface techniques in electroanalytical chemistry*. *Chemical Analysis (New York)*, 1996. **139**(Modern Techniques in Electroanalysis): p. 1-58.

33. Vickerman, J.C., *Surface analysis – the principal techniques*. 1997: John Wiley & Sons.
34. Ranke, W. (2004) *Modern Methods in Heterogeneous Catalysis Research: Theory and Experiment*. Surface Analysis.
35. Bernasek, F.F.T.a.S.L., ed. *Functionalization of Semiconductor Surfaces*. First Edition ed. 2012, John Wiley & Sons, Inc.
36. Moore, G.E., *Cramming More Components onto Integrated Circuits*. Electronics 1965: p. 114-117.
37. Moffat, T.P., et al., *Electrodeposition of Cu on Ru barrier layers for damascene processing*. Journal of the Electrochemical Society, 2006. **153**(1): p. C37-C50.
38. Andricacos, P.C., et al., *Damascene copper electroplating for chip interconnections*. IBM Journal of Research and Development, 1998. **42**(5): p. 567-574.
39. Guo, L., A. Radisic, and P.C. Searson, *Electrodeposition of copper on oxidized ruthenium*. J. Electrochem. Soc. FIELD Full Journal Title:Journal of the Electrochemical Society, 2006. **153**(12): p. C840-C847.
40. Perng, D.C., J.B. Yeh, and K.C. Hsu, *Phosphorous doped Ru film for advanced Cu diffusion barriers*. Applied Surface Science, 2008. **254**(19): p. 6059-6062.
41. Chan, R., et al., *Diffusion Studies of Copper on Ruthenium Thin Film*. Electrochemical and Solid-State Letters, 2004. **7**(8): p. G154-G157.
42. Arunagiri, T.N., et al., *5 nm ruthenium thin film as a directly plateable copper diffusion barrier*. Applied Physics Letters, 2005. **86**(8).

43. Duong, H.T., et al., *Oxygen Reduction Catalysis of the Pt₃Co Alloy in Alkaline and Acidic Media Studied by X-ray Photoelectron Spectroscopy and Electrochemical Methods*. Journal of Physical Chemistry C, 2007. **111**(36): p. 13460-13465.
44. Kim, J.Y., Y.-G. Kim, and J.L. Stickney, *Cu nanofilm formation by electrochemical atomic layer deposition (ALD) in the presence of chloride ions*. J. Electroanal. Chem. FIELD Full Journal Title:Journal of Electroanalytical Chemistry, 2008. **621**(2): p. 205-213.
45. Burke, L.D., N.S. Naser, and R. Sharna, *The oxide electrochemistry of ruthenium and its relevance to trench liner applications in damascene copper plating*. Journal of Applied Electrochemistry, 2008. **38**(3): p. 377-384.
46. Stickney, J.L., S.D. Rosasco, and A.T. Hubbard, *Electrodeposition of Copper on Pt(111) Surfaces Pretreated with Iodine. Studies by LEED, Auger Spectroscopy and Electrochemistry*. J. Electrochem. Soc. , 1984. **131**: p. 260.
47. Liu, J., et al., *The effects of an iodine surface layer on Ru reactivity in air and during Cu electrodeposition*. Journal of The Electrochemical Society, 2005. **152**(2): p. G115-G121.
48. Stickney, J.L., C.B. Ehlers, and B.W. Gregory, *Adsorption of gaseous and aqueous hydrochloric acid on the low-index planes of copper*. Langmuir, 1988. **4**(6): p. 1368-73.
49. Stickney, J.L. and C.B. Ehlers, *Surface chemistry of electrodes: copper(111) in aqueous hydrochloric acid*. Journal of Vacuum Science & Technology, A: Vacuum, Surfaces, and Films, 1989. **7**(3, Pt. 2): p. 1801-5.

50. Ehlers, C.B., I. Villegas, and J.L. Stickney, *The surface chemistry of Cu (100) in HCl solutions as a function of potential: a study by LEED, Auger spectroscopy and depth profiling*. Journal of Electroanalytical Chemistry, 1990. **284**(2): p. 403-412.
51. Andricacos, P.C., *Copper on-chip interconnections*. Interface, 1999. **8**(1): p. 32.
52. Hai, N.T.M., et al., *Combined scanning tunneling microscopy and synchrotron X-ray photoemission spectroscopy results on the oxidative CuI film formation on Cu(111)*. Journal of Physical Chemistry C, 2007. **111**(40): p. 14768-14781.
53. Vereecken, P.M., et al., *The chemistry of additives in damascene copper plating*. Ibm Journal of Research and Development, 2005. **49**(1): p. 3-18.
54. Josell, D., D. Wheeler, and T.P. Moffat, *Gold Superfill in Submicrometer Trenches: Experiment and Prediction*. Journal of The Electrochemical Society, 2006. **153**(1): p. C11-C18.
55. Moffat, T.P., et al., *Superconformal film growth: Mechanism and quantification*. Ibm Journal of Research and Development, 2005. **49**(1): p. 19-36.
56. Kang, M.C., et al., *Local Corrosion of the Oxide Passivation Layer during Cu Chemical Mechanical Polishing*. Electrochemical and Solid State Letters, 2009. **12**(12): p. H433-H436.
57. Ehlers, C.B. and J.L. Stickney, *Surface chemistry of copper(100) in acidic sulfate solutions*. Surface Science, 1990. **239**(1-2): p. 85-102.
58. Kim, J.Y., Y.G. Kim, and J.L. Stickney, *Cu nanofilm formation by electrochemical atomic layer deposition (ALD) in the presence of chloride ions*. Journal of Electroanalytical Chemistry, 2008. **621**(2): p. 205-213.

59. Chia, V.K.F., et al., *Adsorption and orientation of hydroquinone and hydroquinone sulfonate at platinum electrodes. Studies by thin-layer electrochemistry, LEED, Auger and infrared spectroscopy.* Journal of Electroanalytical Chemistry and Interfacial Electrochemistry, 1984. **163**(1-2): p. 407-13.
60. Stickney, J.L., S.D. Rosasco, and A.T. Hubbard, *Electrodeposition of Copper on Pt(111) Surfaces Pretreated with Iodine. Studies by LEED, Auger Spectroscopy and Electrochemistry.* JECS, 1983. **131**: p. 260.
61. An, K.S., et al., *Epitaxial growth of Sb thin film and chemical reaction of Sb-induced surface reconstruction on Si(1 1 3)3×2.* Surface Science, 2001. **492**(1-2): p. L705-L710.
62. Haller, E.E., *Germanium: From its discovery to SiGe devices.* Materials Science in Semiconductor Processing, 2006. **9**(4-5): p. 408-422.
63. Rivillon, S., R.T. Brewer, and Y.J. Chabal, *Water reaction with chlorine-terminated silicon (111) and (100) surfaces.* Applied Physics Letters, 2005. **87**(17).
64. C. O. Chui, H.K., D. Chi, B. B. Triplett, P. C. McIntyre and K. C. Saraswat, IEDM 2002 Tech. Dig., 2002: p. 437.
65. Nylandsted Larsen, A., *Epitaxial growth of Ge and SiGe on Si substrates.* Materials Science in Semiconductor Processing, 2006. **9**(4-5): p. 454-459.
66. Van Elshocht, S., et al., *Study of CVD high-k gate oxides on high-mobility Ge and Ge/Si substrates.* Thin Solid Films, 2006. **508**(1-2): p. 1-5.

67. Brunco, D.P., et al., *Germanium: The Past and Possibly a Future Material for Microelectronics*. ECS Transactions, 2007. **11**(4): p. 479-493.
68. Bellenger, F., et al., *Electrical Passivation of the (100)Ge Surface by Its Thermal Oxide*. ECS Transactions, 2007. **11**(4): p. 451-459.
69. Endres, F. and S. Zein El Abedin, *Nanoscale electrodeposition of germanium on Au(111) from an ionic liquid: an in situ STM study of phase formation. Part I. Ge from GeBr₄*. Physical Chemistry Chemical Physics, 2002. **4**(9): p. 1640-1648.
70. Lokhande, C.D. and S.H. Pawar, *ELECTRODEPOSITION OF THIN-FILM SEMICONDUCTORS*. Physica Status Solidi a-Applied Research, 1989. **111**(1): p. 17-40.

CHAPTER 2
ELECTROCHEMICAL ATOMIC LAYER DEPOSITION OF COPPER NANOFILMS
ON RUTHENIUM¹

¹ D. K. Gebregziabiher, Y. G. Kim, C. Thambidurai V. Ivanova, P. H. Haumesser, J. L. Stickney, *Journal of Crystal Growth* 312 (2010) 1271–1276.

Reprinted here with permission of publisher

Abstract

As ULSI scales to smaller and smaller dimensions, it has become necessary to form layers of materials only a few nm thick. Substrates now support trenches, while deposits of some materials must be conformal. Atomic layer deposition (ALD) is being developed to address such issues. ALD is the formation of materials layer by layer using self-limiting reactions. This article describes the formation of Cu seed layers (for the Cu Damascene process) on a Ru barrier layer. The deposit was formed by the electrochemical analog of ALD, using electrochemical self-limiting reactions which are referred to as underpotential deposition (UPD). A linear dependence was shown for Cu growth over 8 ALD cycles, and STM showed a conformal deposition, as expected for an ALD process. Relative Cu coverages were determined using Auger electron spectroscopy, while absolute Cu coverages were obtained from coulometry during oxidative stripping of the deposits. Use of a Cl⁻ containing electrolyte results in Cu deposits covered with an atomic layer of Cl atoms, which have been shown to protect the surface from oxidation during various stages of the deposition process. The 10 nm thick Ru substrates were formed on Si(100) wafers, and were partially oxidized upon receipt. Electrochemical reduction, prior to Cu deposition, removed the oxygen and some traces of carbon, the result of transport. Ion bombardment proved to clean all oxygen and carbon traces from the surface.

Key Words: UPD, ALD, electrochemical-ALD, seed layers, liners.

Introduction

The Damascene process for deposition of Cu interconnects must scale, as does everything else in microelectronics, according to Moore's law [1]. Damascene Cu deposition for the Back End (everything except the first layer of transistors in ULSI) requires a liner to prevent inter-diffusion of Cu, and to facilitate Cu electrodeposition [2-4]. Presently, Ta/TaN diffusion barriers are used to isolate Cu from the dielectric material. Direct electrodeposition of Cu on such barriers is difficult, so a seed layer of Cu, formed by physical vapor deposition (PVD), is generally inserted between the barrier layer and the Damascene Cu [2-4] to complete the liner. However, obtaining a conformal Cu seed layer by PVD can be difficult in very low dimensions or high aspect ratios, resulting in problems such as uneven filling of trenches and vias: holes and defects in the deposit. The use of Cu in the Back End was adopted to enhance IC performance by reducing RC delay times [5]. However, as the feature size decreased, and aspect ratios increased, new challenges were created to the deposition of conformal liners [2].

Ruthenium has lower thermal and electrical resistivity when compared to Ta/TaN and its low solubility in copper makes it a candidate for Cu metallization barrier layers. Perng et al. reported that ultra-thin ruthenium is stable as a barrier layer up to 300⁰C and suggested that doping the ruthenium with phosphorus may help its barrier properties at higher temperatures, even though the sheet resistance increases slightly [5]. Another advantage of ruthenium as a barrier layer is that it has strong adhesion to Cu, which can then be directly plated. Chan et al reported that a 20 nm ruthenium barrier layer can prevent copper diffusion up to a temperature of 450⁰C [6] and Arunagiri et al. demonstrated that 5nm ruthenium can act as a platable Cu diffusion barrier up to 300⁰C

[7]. According to Wei et al. Cu starts to diffuse through 1nm ruthenium around 300⁰C [8]. Soo et al. reported that ALD-Ru (4nm)/ALD-TaCN (2nm) prevented copper diffusion up to 550⁰C and increasing the ALD-Ru to 12nm prevented the diffusion of copper up to a temperature of 600⁰C for 30 minutes [9].

One problem with ruthenium is that it is susceptible to oxidation in air and aerated water, if not passivated with copper. Moffat et al. claim that the presence of an oxide results in weak Cu-Ru adhesion and may even prevent copper under potential deposition (UPD) [2, 10]. They also claim that the deposition of copper occurs competitively with oxide reduction, which may control its deposition kinetics. They suggest that the 3-D oxide can be reduced by polarizing the ruthenium near the hydrogen evolution region [2] prior to exposure to the Cu solution.

Stickney et al have demonstrated that adsorbing I atoms on some metal surfaces prevents surface contamination and oxidation under ambient conditions [11]. Kelber et al. reported that adsorbing I atoms from I₂ at 300K passivated a ruthenium surface against oxidation. In addition, during overpotential Cu electrodeposition (OPD), the I atoms floated on top of the depositing Cu, thus maintaining the protection as the deposit grew [12]. The Stickney group has also studied the adsorption of Cl on Cu single crystal surfaces, where it was also shown to protect the surface, while forming a well ordered atomic layer [13-15].

In the study reported here, the growth of Cu films on 10 nm of electron beam evaporated Ru (on a Si(100) wafer) was performed using the electrochemical form of atomic layer deposition (EC-ALD) [16-18] [19-23]. ALD is the layer by layer formation of nanofilms, using surface limited reactions in a cycle [24-28]. Underpotential

deposition (UPD) is a name for an electrochemical surface limited reaction, a phenomenon where an atomic layer of one element can form on a second element at a potential prior to, under, that needed to deposit the element on itself [29-34]. This results from the free energy of formation of a surface compound or alloy. The potential can be selected so that only an atomic layer of the first metal is formed, and no more, no bulk deposit of that element. The electrochemical form of ALD results from the combination of UPD with ALD, although it was originally referred to as electrochemical atomic layer epitaxy (EC-ALE) for historical reasons [35].

The deposition of Cu films in this study started with direct underpotential deposition (UPD) of Cu on the 10nm Ru film, on Si, as the first cycle in Cu ALD. A second atomic layer of Cu could not be formed by the same method, UPD, given the definition above, as there would be no energetic advantage for the formation of a Cu layer on a Cu layer, relative to bulk Cu deposition. In order to form the second and subsequent atomic layers of Cu, monolayer galvanic displacement [36, 37], also referred to as surface limited redox replacement [23, 38-42] was used. That is, since UPD Cu cannot be formed on Cu, to obtain a limited reaction an atomic layer of a different element (less noble, or more reactive) was first formed via UPD (the sacrificial layer). Next, a solution containing ions of the desired element, Cu^{2+} , was introduced, and allowed to exchange by redox replacement for the sacrificial element. The limited nature of this process comes from the amount of the sacrificial element deposited as an atomic layer from UPD, which can only deliver a fixed and finite number of electrons. That number of electrons stipulates the maximum amount of Cu that can be formed in a cycle: Faraday's 1st law of electrolysis.

In the present studies, Pb UPD was used to form the sacrificial layers. The Pb^{2+} solution was then replaced with a Cu^{2+} solution, facilitating exchange of Pb for Cu. This constituted one ALD cycle and was repeated up to seven times, in these studies. This concept of surface limited redox replacement was inspired by the work of Adzic, Brankovic, and Wang [43] who were using “monolayer galvanic replacement” to form fractions of a monolayer of Pt, in studies of fuel cell catalyst reactions. The late Mike Weaver et al. repeated that process, performing up to 8 cycles, in what appears to be the first example of electrochemical ALD of a pure element [37]. The process of surface limited redox replacement has been described in more depth elsewhere [44-46].

The present investigation made use of an ultra-high vacuum (UHV) surface analytical instrument, in combination with electrochemical experiments performed within an ante-chamber of the instrument, in a process referred to as UHV-EC [47, 48]. This study demonstrated that a Cu seed layer can be formed by electrochemical ALD directly on a Ru diffusion barrier.

Experimental

The Si(100) wafer coated with 10nm Ru, formed by electron beam evaporation, was obtained from LETI (Grenoble, France). The as received substrate was cleaned using cyclic voltammetry in degassed 10mM HClO_4 (Aldrich, doubly distilled), to remove the oxide layer formed in transit. The electrochemical experiments were performed in a SS ante-chamber on the UHV instrument. The ante-chamber was back filled to atmospheric pressure with high purity Ar-gas (99.999%) while the electrochemical experiments were performed. Subsequently, the electrochemical cell was removed from the ante-chamber through a 4.5” gate valve, and the ante-chamber was

pumped down so the sample could be transferred to the main analysis chamber for characterization, without exposure to air. The substrate was further cleaned by Ar⁺ ion bombardment to remove any remaining contaminants. The analysis chamber was also equipped with optics for low energy electron diffraction (LEED) (Princeton Research Instruments, Inc.) and a cylindrical mirror analyzer for Auger Electron Spectroscopy (AES) (Perkin-Elmer). Scanning tunneling microscopy (STM) studies were performed in solution, using a Nanoscope 3 (Veeco).

The solutions used were 0.1mM Cu(ClO₄)₂ (Aldrich, 98%) in 2.5 mM HCl (Sigma Aldrich) and 1.0 mM Pb(ClO₄)₂ (Aldrich, 99.995%) in 2.5 mM HCl, where the pH was adjusted to 4.4 using NaOH (J. T. Baker). The electrochemical reactions were performed in a Pyrex cell with an Au-wire counter electrode and an Ag/AgCl (3M KCl) reference electrode (BioAnal). A μ Autolab Type III Potentiostat/Galvanostat was used for potential control. All potentials were reported vs Ag/AgCl (3M KCl).

The solutions were degassed with high purity Ar-gas for one hour prior to the electrochemical studies. Cu UPD was performed, for 1 min, to form the first Cu atomic layer. It was followed by the deposition of Pb UPD @ -0.475V for 1min, to form the sacrificial atomic layer. Pb UPD on Cu UPD was then exposed to the Cu²⁺ solution, at its open circuit potential (OCP) for the redox exchange, completing one ALD cycle. That cycle was used to grow Cu nanofilms using 2, 3, 5 and 7 cycles. Cyclic voltammetry, current time transients, scanning tunneling microscopy (STM) and Auger electron spectroscopy (AES) were used to investigate the deposition process.

Results and Discussion

Cleaning the substrate

Auger electron spectra (AES) of the as received 10nm Ru film, on the Si(100) substrate, indicated the presence of oxygen (Figure 2.1). Figure 2.2 shows CVs of the as received sample in 10 mM HClO₄, at a scan rate of 5mV/s. The scans began with immersion of the sample at 0.353 V, its OCP. It was initially scanned negative to -0.4V, where the scan direction was reversed and the potential scanned to 0.4V (dotted curve). A broad reduction feature that started at 0.1V and peaked at -0.1 V, during the first negative going scan, corresponds to Ru surface oxide reduction [2]. That feature was not present in subsequent scans, suggests that the surface oxide layer was reduced on the first scan, and was not reformed by oxidation to 0.4 V. The substrate was emersed (withdrawn from solution) at -0.22V, and transferred to the analysis chamber. AES of the sample (Figure 2.1) showed nearly complete loss of the oxygen signal, consistent with electrochemical reduction of the oxide. The substrate was then bombarded with Ar⁺ ions to remove any remaining contaminants, and the cleanliness was confirmed using AES Figure 2.1. There is a problem with measuring the coverage of C on a Ru surface with Auger. That is, both C and Ru have essentially the same transition energy. However, by taking the ratio of the positive (p) to the negative (n) excursions of the 270eV Ru Auger feature, a measure of the extent of C contamination can be determined, according to Goodman et al.[49], so that this ratio can be used to determine when the surface is clean. Because the carbon 273eV peak overlaps that for ruthenium, the p excursion tends to be smaller when the surface is dirty. When it is clean, the ratio is generally over 0.7, as it is in Figure 1. for the “after cold ion bombardment” spectrum, where it is measured

as 0.75. The presence of C is clearly evident, by this measure, for the as received sample and that after electrochemistry, although the electrochemistry did appear to clean it significantly.

Electrochemical Deposition of Copper

The clean Ru sample was then transferred to the ante-chamber where a first atomic layer of copper was deposited in two ways: First; Pb UPD was formed on the Ru, and then redox replaced using a Cu^{2+} solution at OCP. Second; Cu UPD was formed on the clean Ru by immersing it in a solution of 0.1mM $\text{Cu}(\text{ClO}_4)_2$ and 2.5mM HCl, at -0.2V, for 1 minute. Auger of these two first atomic layers, after transfer back to the analysis chamber, showed the presence of Cu, Cl, and Ru, as well as a small amount of O on the surface. Slightly more oxygen was evident if the first Cu layer was formed by redox replacement of Pb, rather than Cu UPD, so Cu UPD on the Ru surface was used in subsequent deposits as the first Cu atomic layer (Figure 2.3, 1st cycle). However, the amount of oxygen observed was very low, given that Cu reacts rapidly with oxygen, even the traces in the high purity Ar or in solution, as oxygen's sticking coefficient is close to 1 for the first monolayer [50]. However, significant oxygen was not observed, in the present study because of the presence of Cl^- in solution. It is well known that Cl adsorbs strongly on Cu in solution, and can protect it from oxidation by ambient oxygen [9, 13, 15, 51].

Different supporting electrolyte concentrations, as well as solution pHs were investigated. With low pH, acid, the Ru nanofilms were easily delaminated during the deposition process. Higher pH solution did not appear to delaminate, and a pH of 4 – 4.5

was selected for the deposition process. For pH values above 5, both Cu^{2+} and Pb^{2+} tended to precipitate as the hydroxides.

Figure 2.3 displays a series of Auger spectra, as a function of the number of Cu ALD cycles performed. Figure 2.4 displays plots of the AES ratios for Cu/Ru and O/Ru as a function of the number of cycles. Overall, the signal for Cu increased steadily, as expected, suggesting an increasing Cu layer thickness. The small amount of the O/Ru signal remained nearly constant (Figure 2.4). Neither of the ratio plots in Figure 4 was smooth, partly because the Ru signal, used to normalize both the Cu and O signals, decreasing as the Cu coverage increased: the Ru Auger electrons were scattered by the increasing Cu film.

On the other hand, the AES ratio of Cu/Cl (Figure 2.5), showed a very monotonic increase with increasing numbers of cycles. It is known that the Cl forms an essentially close packed layer on a Cu surface [13, 14, 51], and that only a single atomic layer will be present. It has also been shown that the Cl will stay on top as the film as it grows, so the signal from that top layer of Cl can be used as an internal standard for Auger analysis. Thus the ratio of Cu/Cl (Figure 2.5) is an accurate relative measure of the deposit thickness, up to a couple of Cu monolayers. At that point, the Cu Auger electrons begin to undergo self-scattering in the thickening Cu layer.

STM images (Figure 2.6) of the clean substrate and after 6 ALD cycles (Cu UPD followed by five cycles of Pb UPD replaced by Cu) show no evidence of a change in morphology, at this scale. The deposit looks essentially the same as the substrate, suggesting a conformal Cu deposit, as expected for an ALD process. The absolute coverage of the deposit was determined by performing anodic stripping in a blank

solution (10mM HClO₄) at 0.15V. The average deposited amount of Cu per cycle was 0.5 ML for each cycle as can be seen from Figure 2.7.

The OCP was used to monitor the exchange of Cu for Pb, each cycle (Figure 2.8). The steady state OCP was generally reached when the Pb had been completely replaced. It can be seen in Figure 2.8 that the steady state OCP shifted to lower potentials over the first few cycles, as the controlling equilibrium shifted from Cu²⁺ ions in equilibrium with Cu UPD to Cu²⁺ ions in equilibrium with bulk Cu. In Figure 2.8, the OCP appears to stabilize between -0.07 and -0.08 V after the first three cycles. This is consistent with the deposition of only about 0.5 ML per cycle, so that equilibrium vs. bulk Cu takes three cycles.

Conclusion

This paper reports the growth of Cu nanofilms on 10nm Ru films, formed on Si (100), by electrochemical ALD. In this study, monolayer galvanic displacement or surface limited redox replacement was used to form the atomic layers. Pb UPD was used to form the sacrificial layers, which were then replaced with Cu from a Cu²⁺ solution. A linear dependence was shown for Cu growth over 8 ALD cycles, and STM showed a conformal deposit, as expected for an ALD process. Relative Cu coverages were determined using Auger electron spectroscopy, while absolute Cu coverages were obtained from coulometry during oxidative stripping of the deposits. Use of a Cl⁻ containing electrolyte resulted in Cu deposits covered with an atomic layer of Cl atoms, which have been shown to protect the surfaced from oxidation, which proved helpful at various stages of the deposition process.

Acknowledgments

Support of this work was from the National Science Foundation, DMR, which is gratefully acknowledged.

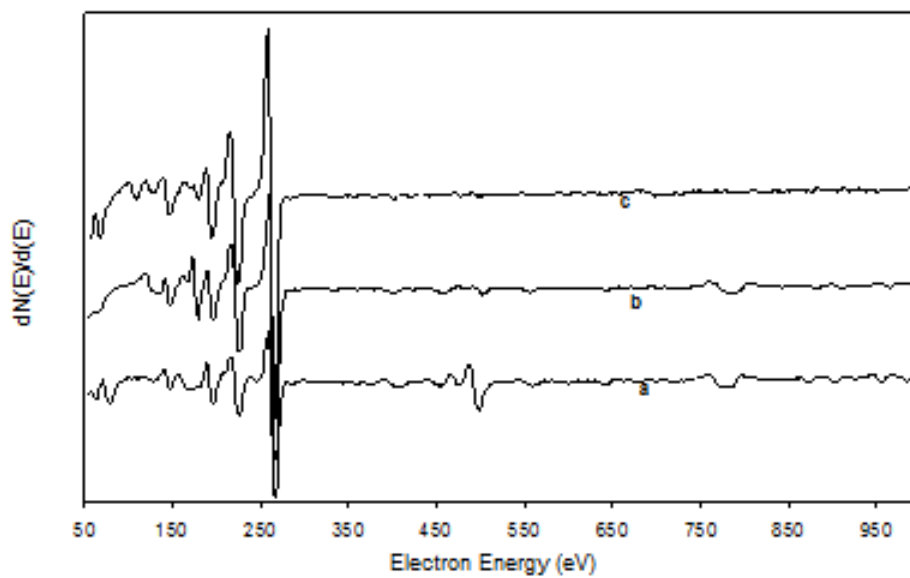


Figure 2.1. Auger spectra of (a) as received 10nm Ru on Si, (b) after CV in 10mM HClO₄ at 5mV/s and (c) after cold ion bombardment for 10 minutes

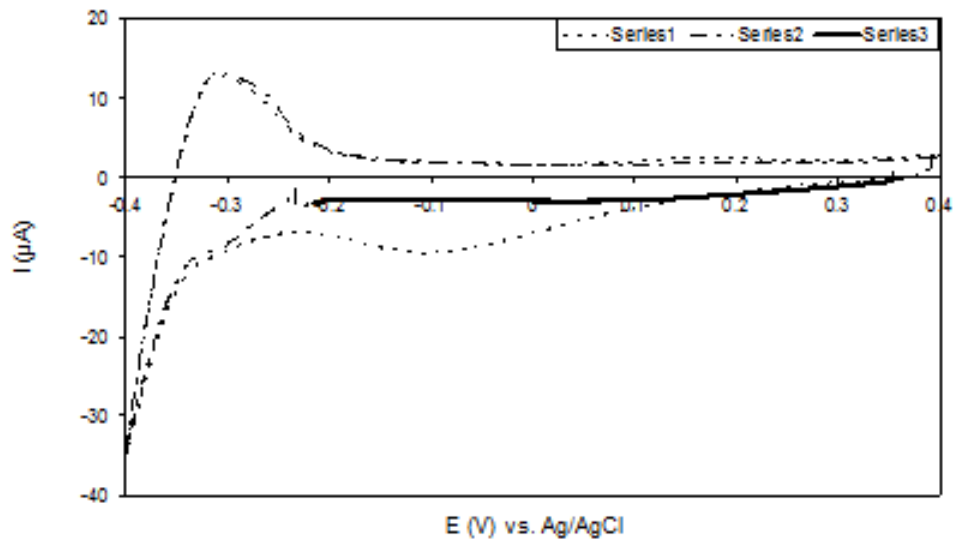


Figure 2.2. CV of 10nm Ru on Si in 10mM HClO₄ at a scan rate of 5mV/s

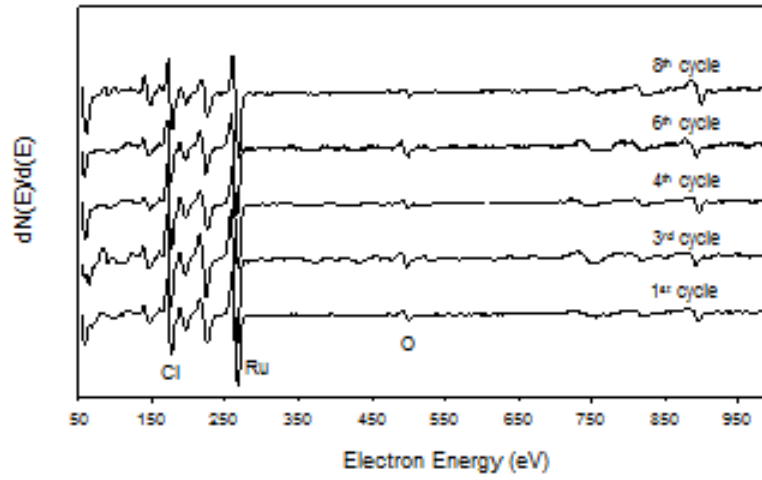


Figure 2.3. Auger spectra of Cu deposition at different cycles

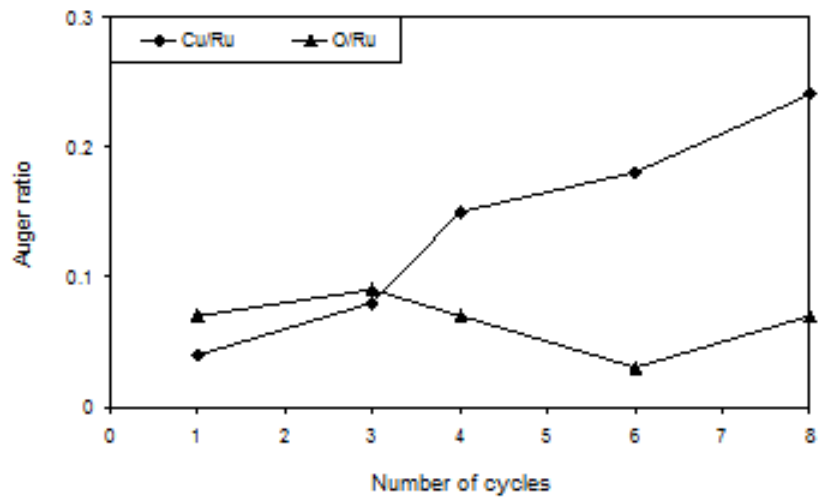


Figure 2.4. Auger peak to peak ratio of atoms vs. the number of cycles

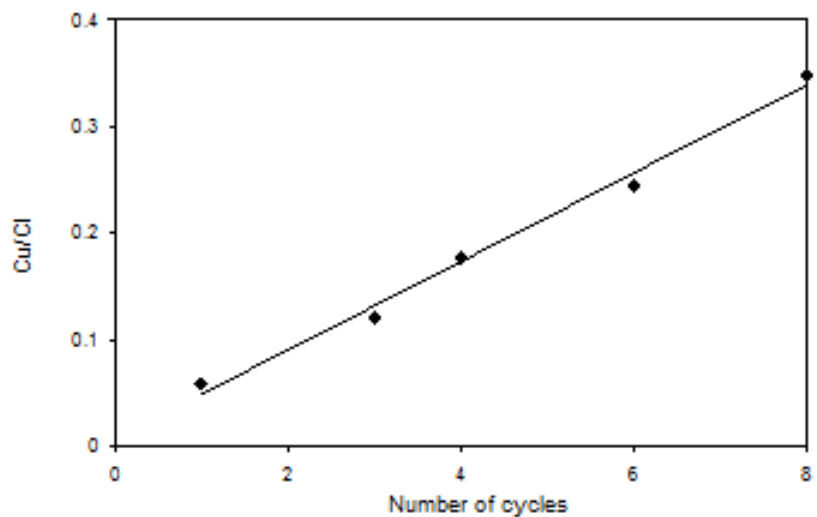


Figure 2.5. Auger ratio of Cu and Cl vs. the number of cycles

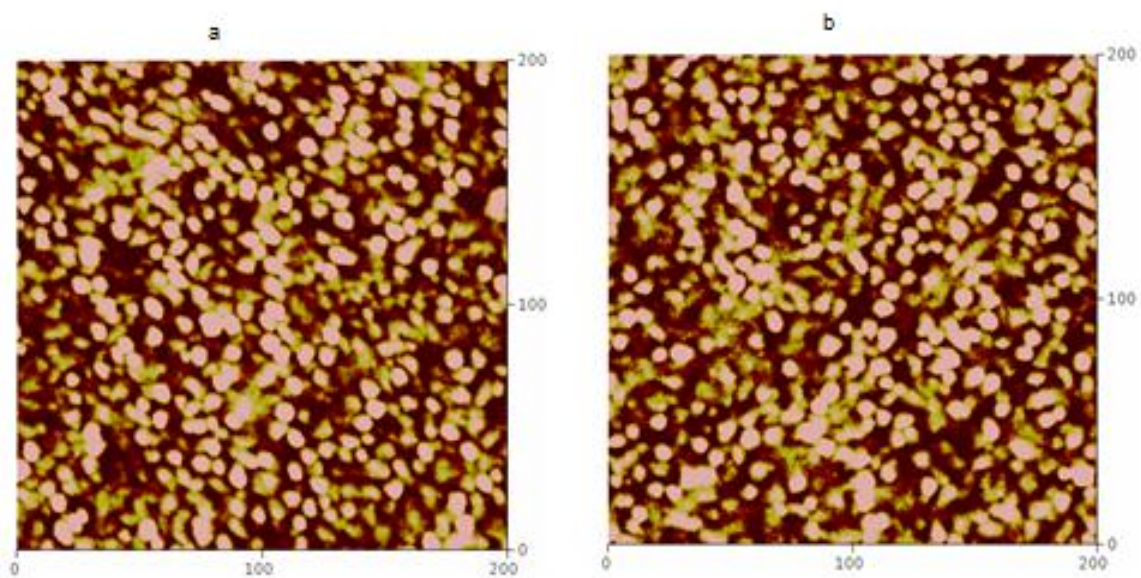


Figure 2.6. STM images of (a) clean 10nm Ru on Si and (b) Cu UPD and 5 cycles of Cu on 10nm Ru on Si

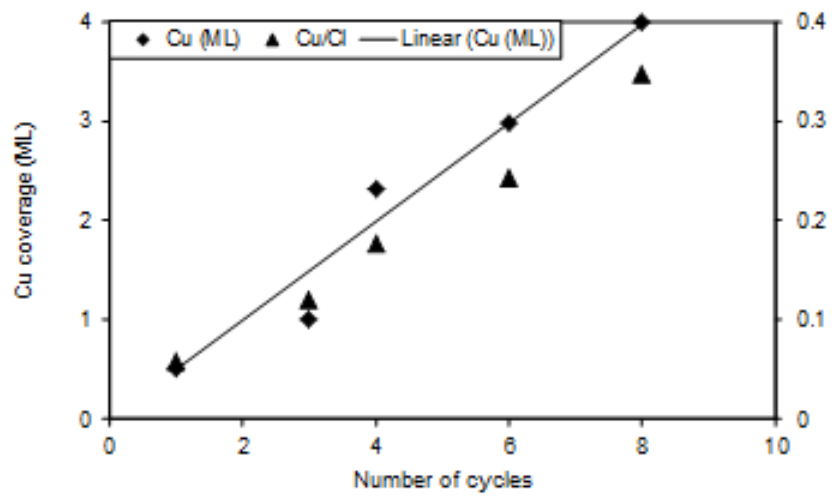


Figure 2.7. Auger peak to peak ratio of Cu to Cl and coverage of Cu vs. number of cycles

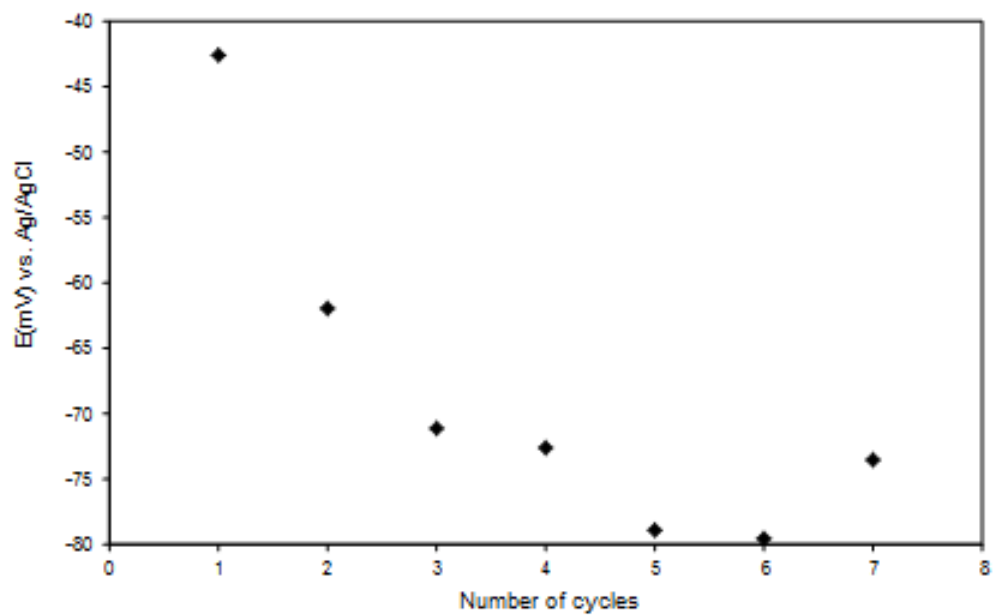


Figure 2.8. Average OCP after successive Cu replacement cycles in 0.1mM $\text{Cu}(\text{ClO}_4)_2$ solution

References

1. Moore, G.E., *Cramming More Components onto Integrated Circuits*. Electronics 1965: p. 114-117.
2. Moffat, T.P., et al., *Electrodeposition of Cu on Ru barrier layers for damascene processing*. Journal of the Electrochemical Society, 2006. **153**(1): p. C37-C50.
3. Andricacos, P.C., et al., *Damascene copper electroplating for chip interconnections*. IBM Journal of Research and Development, 1998. **42**(5): p. 567-574.
4. Guo, L., A. Radisic, and P.C. Searson, *Electrodeposition of copper on oxidized ruthenium*. J. Electrochem. Soc. FIELD Full Journal Title:Journal of the Electrochemical Society, 2006. **153**(12): p. C840-C847.
5. Perng, D.C., J.B. Yeh, and K.C. Hsu, *Phosphorous doped Ru film for advanced Cu diffusion barriers*. Applied Surface Science, 2008. **254**(19): p. 6059-6062.
6. Chan, R., et al., *Diffusion Studies of Copper on Ruthenium Thin Film*. Electrochemical and Solid-State Letters, 2004. **7**(8): p. G154-G157.
7. Arunagiri, T.N., et al., *5 nm ruthenium thin film as a directly plateable copper diffusion barrier*. Applied Physics Letters, 2005. **86**(8).
8. Duong, H.T., et al., *Oxygen Reduction Catalysis of the Pt3Co Alloy in Alkaline and Acidic Media Studied by X-ray Photoelectron Spectroscopy and Electrochemical Methods*. Journal of Physical Chemistry C, 2007. **111**(36): p. 13460-13465.
9. Kim, J.Y., Y.-G. Kim, and J.L. Stickney, *Cu nanofilm formation by electrochemical atomic layer deposition (ALD) in the presence of chloride ions*. J.

- Electroanal. Chem. FIELD Full Journal Title:Journal of Electroanalytical Chemistry, 2008. **621**(2): p. 205-213.
10. Burke, L.D., N.S. Naser, and R. Sharna, *The oxide electrochemistry of ruthenium and its relevance to trench liner applications in damascene copper plating*. Journal of Applied Electrochemistry, 2008. **38**(3): p. 377-384.
 11. Stickney, J.L., S.D. Rosasco, and A.T. Hubbard, *Electrodeposition of Copper on Pt(111) Surfaces Pretreated with Iodine. Studies by LEED, Auger Spectroscopy and Electrochemistry*. J. Electrochem. Soc. , 1984. **131**: p. 260.
 12. Liu, J., et al., *The effects of an iodine surface layer on Ru reactivity in air and during Cu electrodeposition*. Journal of The Electrochemical Society, 2005. **152**(2): p. G115-G121.
 13. Stickney, J.L., C.B. Ehlers, and B.W. Gregory, *Adsorption of gaseous and aqueous hydrochloric acid on the low-index planes of copper*. Langmuir, 1988. **4**(6): p. 1368-73.
 14. Stickney, J.L. and C.B. Ehlers, *Surface chemistry of electrodes: copper(111) in aqueous hydrochloric acid*. Journal of Vacuum Science & Technology, A: Vacuum, Surfaces, and Films, 1989. **7**(3, Pt. 2): p. 1801-5.
 15. Ehlers, C.B., I. Villegas, and J.L. Stickney, *The surface chemistry of Cu (100) in HCl solutions as a function of potential: a study by LEED, Auger spectroscopy and depth profiling*. Journal of Electroanalytical Chemistry, 1990. **284**(2): p. 403-412.

16. Gregory, B.W., D.W. Suggs, and J.L. Stickney, *Conditions for the deposition of cadmium telluride (CdTe) by electrochemical atomic layer epitaxy*. Journal of the Electrochemical Society, 1991. **138**(5): p. 1279-84.
17. Colletti, L.P., B.H. Flowers, and J.L. Stickney, *Formation of Thin-Films of CdTe, CdSe, and CdS by Electrochemical ALE*. JECS, 1997.
18. Foresti, M.L., et al., *Electrochemical atomic layer epitaxy deposition of CdS on Ag (111): An electrochemical and STM investigation*. Journal of Physical Chemistry B, 1998. **102**(38): p. 7413-7420.
19. Villegas, I., *TEM of CdTe formed by electrochemical ALE*. JACS, 1998. **submitted**.
20. Pezzatini, G., et al., *Formation of ZnSe on Ag(111) by electrochemical atomic layer epitaxy*. Journal of Electroanalytical Chemistry, 1999. **475**(2): p. 164-170.
21. Zou, S. and M.J. Weaver, *Surface-enhanced Raman spectroscopy of cadmium sulfide/cadmium selenide superlattices formed on gold by electrochemical atomic-layer epitaxy*. Chemical Physics Letters, 1999. **312**(2-4): p. 101-107.
22. Torimoto, T., et al., *Photoelectrochemical activities of ultrathin PbS films prepared by electrochemical atomic layer epitaxy*. JEC, 2000. **submitted**.
23. Kim, Y.G., et al., *Platinum nanofilm formation by EC-ALE via redox replacement of UPD copper: Studies using in-situ scanning tunneling microscopy*. Journal of Physical Chemistry B, 2006. **110**(36): p. 17998-18006.
24. George, S.M., J.D. Ferguson, and J.W. Klaus, *Atomic layer deposition of thin films using sequential surface reactions*. Materials Research Society Symposium

- Proceedings, 2000. **616**(New Methods, Mechanisms and Models of Vapor Deposition): p. 93-101.
25. Ritala, M. and M. Leskela, *Atomic layer deposition*. Handbook of Thin Film Materials, 2002. **1**: p. 103-159.
 26. Gordon, R.G., *Review of recent progress in atomic layer deposition (ALD) of materials for micro- and nano-electronics*. PMSE Preprints, 2004. **90**: p. 726-728.
 27. Ritala, M., *Atomic layer deposition*. High-k Gate Dielectrics, 2004: p. 17-64.
 28. Shen, C., X.-y. Liu, and G.-z. Huang, *Atomic layer deposition and its applications in semiconductor*. Zhenkong, 2006. **43**(4): p. 1-6.
 29. Kolb, D.M., *Physical and Electrochemical Properties of Metal Monolayers on Metallic Substrates*, in *Advances in Electrochemistry and Electrochemical Engineering*, H. Gerischer and C.W. Tobias, Editors. 1978, John Wiley: New York. p. 125.
 30. Juttner, K. and W.J. Lorenz, *Underpotential Metal Deposition on Single Crystal Surfaces*. Z. Phys. Chem. N. F., 1980. **122**: p. 163.
 31. Adzic, R.R., *Electrocatalytic Properties of the Surfaces Modified by Foreign Metal Ad Atoms*, in *Advances in Electrochemistry and Electrochemical Engineering*, H. Gerischer and C.W. Tobias, Editors. 1984, Wiley-Interscience: New York. p. 159.
 32. Gewirth, A.A. and B.K. Niece, *Electrochemical applications of in situ scanning probe microscopy*. Chem. Rev., 1997. **97**: p. 1129-1162.

33. Herrero, E., L.J. Buller, and H.D. Abruna, *Underpotential Deposition at Single Crystal Electrodes Surfaces of Au, Pt, Ag and other Materials*. Chemical Reviews, 2001. **101**: p. 1897-1930.
34. Magnussen, O.M., *Ordered anion adlayers on metal electrode surfaces*. Chemical Reviews, 2002. **102**(3): p. 679-725.
35. Gregory, B.W. and J.L. Stickney, *Electrochemical atomic layer epitaxy (ECALE)*. Journal of Electroanalytical Chemistry, 1991. **300**(1-2): p. 543-561.
36. Brankovic, S.R., J.X. Wang, and R.R. Adzic, *Metal monolayer deposition by replacement of metal adlayers on electrode surfaces*. SS, 2001. **474**: p. L173-L179.
37. Mrozek, M.F., Y. Xie, and M.J. Weaver, *Surface-enhanced Raman scattering on uniform platinum-group overlayers: Preparation by redox replacement of underpotential-deposited metals on gold*. Analytical Chemistry, 2001. **73**(24): p. 5953-5960.
38. Thambidurai, C., Y.-G. Kim, and J.L. Stickney, *Electrodeposition of Ru by atomic layer deposition (ALD)*. Electrochimica Acta, 2008. **53**(21): p. 6157-6164.
39. Kim, J.Y., Y.G. Kim, and J.L. Stickney, *Copper nanofilm formation by electrochemical atomic layer deposition - Ultrahigh-vacuum electrochemical and in situ STM studies*. Journal of the Electrochemical Society, 2007. **154**(4): p. D260-D266.
40. Kim, J.Y., Y.-G. Kim, and J.L. Stickney, *Studies of Cu Atomic Layer Replacement, formed by Underpotential deposits, to Form Pt Nanofilms Using*

- Electrochemical Atomic Layer Epitaxy (EC-ALE)*. ECS Transactions, 2006. **1**(30): p. 41-48.
41. Dimitrov, N., R. Vasilic, and N. Vasiljevic, *A Kinetic Model for Redox Replacement of UPD Layers*. Electrochemical and Solid-State Letters, 2007. **10**(7): p. D79-D83.
 42. Vasilic, R., L.T. Viyannalage, and N. Dimitrov, *Epitaxial growth of Ag on Au(111) by galvanic displacement of Pb and Tl monolayers*. Journal of the Electrochemical Society, 2006. **153**(9): p. C648-C655.
 43. Brankovic, S.R., J.X. Wang, and R.R. Adzic, *New methods of controlled monolayer-to-multilayer deposition of Pt for designing electrocatalysts at an atomic level*. Journal of the Serbian Chemical Society, 2001. **66**(11-12): p. 887-898.
 44. Jeong, S.W., et al., *Effects of annealing temperature on the characteristics of ALD-deposited HfO₂ in MIM capacitors*. Thin Solid Films, 2006. **515**(2): p. 526-530.
 45. Vasilic, R. and N. Dimitrov, *Epitaxial Growth by Monolayer-Restricted Galvanic Displacement*. Electrochemical and Solid-State Letters, 2005. **8**(11): p. C173-C176.
 46. Brankovic, S.R., J. McBreen, and R.R. Adzic, *Spontaneous deposition of Pt on the Ru(0001) surface*. Journal of Electroanalytical Chemistry, 2001. **503**(1-2): p. 99-104.
 47. Hubbard, A.T., *Accounts of Chemical Research*, 1980. **13**: p. 177.

48. Soriaga, M.P. and J.L. Stickney, *Vacuum surface techniques in electroanalytical chemistry*. Chemical Analysis (New York), 1996. **139**(Modern Techniques in Electroanalysis): p. 1-58.
49. Goodman, D.W. and J.M. White, *Measurement of active carbon on ruthenium (110): Relevance to catalytic methanation*. Surface Science, 1979. **90**(1): p. 201-203.
50. Stickney, J.L., C.B. Ehlers, and B.W. Gregory, *Surface chemistry of copper electrodes: preliminary studies*. ACS Symposium Series, 1988. **378**(Electrochem. Surf. Sci.: Mol. Phenom. Electrode Surf.): p. 99-110.
51. Stickney, J.L., B.W. Gregory, and C. Ehlers, *Surface Studies of the Absorption of Aqueous and Gaseous Hcl on the Low Index Planes of Copper*. Journal of the Electrochemical Society, 1988. **135**(3): p. C158-C158.

CHAPTER 3

Cu(111) SURFACE PASSIVATION WITH ATOMIC LAYERS OF Te, Se OR I, STUDIED USING AUGER SPECTRSCOPY²

² Daniel K. Gebregziabher, Maria A. Ledina, Robert Preisser and John L. Stickney, *Journal of The Electrochemical Society*, **159** (8) H675-H679 (2012)

Reprinted here with permission of publisher

Abstract

Efforts are described to identify an atomic layer (AL) passivating agent for Cu, allowing it to be transferred from solution, between solutions, or from solution into vacuum without oxidation. Atomic layers investigated included tellurium, selenium and iodine. Potentials and pH used to form the AL were investigated. Elemental ratios from auger electron spectroscopy (AES), such as O/Cu, and low energy electron diffraction (LEED) patterns were used to characterize the Te, Se and I AL before and after exposure to oxygen. The AL for all three elements resulted in $1/3$ ML coverage ($\sqrt{3}\times\sqrt{3}$)R30° structures.

The ability of an AL to passivate the Cu(111) surface was investigated by exposing it to solution vapor in 1 atm of UHP Ar for 5 minutes within the EC ante-chamber. The resulting surface was then characterized in the analysis chamber. The intent was to mimic transfer between tools in a FAB. In addition, AL coated Cu(111) substrates were exposed to atmospheric oxygen for over 10 minutes, followed by characterization. Exposure to solution vapor and 1 atm UHP Ar resulted in no significant oxygen uptake, though small oxygen signals were detected for the Se AL and the I AL. However, only the Te AL provided passivation to atmospheric oxygen for 10 minutes.

Introduction

Copper is of immense importance in microelectronics, being used for interconnects on the back end of ULSI, as the on-chip wiring material [1-5]. Copper replaced aluminum in integrated circuits as the interconnect material of choice because of its decreased electrical resistance and lower susceptibility to electro-migration [6, 7]. The electrochemical process for Cu on chip wiring is referred to as the Damascene process. Its ability to achieve bottom up filling of vias and high aspect ratio trenches is particularly important to present ULSI designs [5, 6].

Copper is a relatively active metal and readily oxidizes in ambient air, forming a mixture of oxides and hydroxides (i.e. Cu_2O , CuO and $\text{Cu}(\text{OH})_2$) which can build up tensile stress [7]. This oxidation can compromise the deposit's electrical conductivity, causing material degradation. It is therefore of interest to minimize the oxidation of copper between steps on the fab floor. While a wafer is in solution, and under potential control, oxidation is easily avoided, however, when that wafer is moved from one plating bath to the next, it can lose potential control (go open circuit), generally oxidizing to some extent in the aqueous electrolyte plating solutions, unless it is protected from oxidation by passivation during transfer.

Adsorption of halides on metal surfaces has been extensively studied over the years [8-12]. UHV-EC studies by Kim J.Y. et al.[13] have shown that an adsorbed layer of chloride protects copper after emersion (withdrawal) from solution, before pumping to UHV and transferring to the analysis chamber for surface characterization. Iodine adsorbed on metal surfaces can also protect the surfaces from contamination while at the same time acting as a surfactant which allows electrodeposition to proceed.[12, 14].

This paper discusses the protection from oxidation by passivation of copper by adsorption of single atomic layers (AL) of elemental surfactants. Electrochemical deposition of selenium, tellurium or iodine atomic layer on Cu(111) surfaces were studied using cyclic voltammetry to investigate the potential dependence, AES to follow surface composition, and LEED to indicate surface order.

Experimental

The electrochemical experiments were performed in a SS ante-chamber on a UHV surface analysis instrument. The ante-chamber was back-filled to atmospheric pressure with high purity Ar-gas (Air Gas 99.997%) prior to the introduction of the electrochemical cell. Electrochemical reactions were performed in a Pyrex glass cell, using a three electrode control configuration. The working electrode was a Cu(111) single crystal, the counter electrode was Au-wire and an Ag/AgCl (3M KCl) (Bio Analytical Systems) reference electrode was used. A μ Autolab Type III Potentiostat/Galvanostat (Eco Chemie B.V.) was used to control the potentials. All potentials were reported vs Ag/AgCl (3M KCl). Solutions were degassed with high purity Ar (99.997%) for one hour prior to electrochemical studies. The Cu(111) was sonicated in acetone for 30s and rinsed with 18M Ω nanopure DI water prior to insertion into the UHV-EC instrument, and further cleaned by Ar⁺ ion bombardment prior to electrochemical experiments. Figure 3.1 is a typical Auger spectrum after cold and hot ion bombardment. No oxygen signal (500 eV) is evident. The corresponding LEED pattern (60 eV) for the clean Cu(111) surface is displayed in Figure 3.2.

Solutions were all formed using research grade chemicals and 18M Ω nanopure DI water, and were as follows:

1. The acid Te deposition solution consisted of 0.1mM TeO_2 and 50mM H_2SO_4 .
2. The basic Te deposition solution consisted of 0.1mM TeO_2 and 20 mM NaOH.
3. The Se deposition solution was 0.1mM H_2SeO_3 , formed using SeO_2 , and 20mM NaClO_4 .
4. The iodine deposition solution was 10 mM KI solution.

After electrochemical studies, the cell was retracted and the ante-chamber pumped down to UHV. The substrate was then transferred to the analysis chamber for characterization, without exposure to ambient air. The analysis chamber was equipped with optics for LEED, (Princeton Research Instruments, Inc.), a cylindrical mirror analyzer for AES (Perkin-Elmer) and an X-ray source (Staib Instruments) and a hemispherical analyzer (Leybold Heraeus) for X-ray photoelectron spectroscopy (XPS).

Results and Discussion

This report describes a study of Cu surface protection from oxidation by passivation during transfer from aqueous solution by the adsorption of atomic layers (AL) of Te, Se, and I. An AL is a homogeneous distribution of ad-atoms, no more than one atom thick. The term AL does not specify coverage (atoms/cm^2), though by its nature an AL is a monolayer (ML) or less. A ML is defined as one adsorbate atom for each substrate surface atom in this study. The proposed benefit of using an atomic layer, rather than a thicker layer, is that it should provide a minimum perturbation to subsequent processing. Ideally, it would be removed before subsequent deposition, or become incorporated into the deposit without affecting device structure or performance. The electrochemical formation of an AL of one element on a different element in a surface limited reaction is known as underpotential deposition (UPD) [15-20]. In general, UPD

takes place when a less noble element is deposited on a more noble one, at a potential prior to (under) the formal potential (E^0) for deposition of the less noble element on itself.

Tellurium

Based on standard potentials (E^0), vs. SHE, for Te (0.529V) and Cu (0.340V), Te UPD on Cu is not expected or found, as Te is more noble than Cu. At potentials where Cu is stable, bulk Te is as well. Te can be electrodeposited on Cu at an overpotential, however a homogeneous Te AL does not result. If Te is stable on clean Cu, Te will cover the surface after overpotential deposition of a few ML, though not homogeneously.

Figure 3.3 is Te cyclic voltammetry (CV) on a clean, well ordered, Cu(111) single crystal immersed into the basic Te solution. The scan starts negative at 5 mV/s from open circuit potential (OCP), -0.43 V, and is reversed at -1.6 V. Several reduction features are evident in the scan, beginning with a peak near -0.55 V. Previous UHV-EC studies of Cu single crystal substrates by this group have shown that OCP immersion results in the spontaneous generation of some Cu ions as the electrode equilibrates with the near surface solution [8]. The peak at -0.55 V is reduction of near surface Cu ions onto the surface.

Figure 3.4 is a graph of O/Cu and Te/Cu Auger peak height ratios for 1 min immersions of the Cu(111) at different potentials. The relative amounts of adsorbates were inferred from these peak height ratios. This ratio is not an elemental ratio. Each element in Auger has its own peak energy, allowing identification of the element, and its own sensitivity factor, preventing the use of peak ratios as a measurement of the surface atomic ratio. However, the Auger peak ratio for an adsorbate to the substrate can be

used as a relative indication of adsorbate coverage, assuming the substrate peak height is nearly constant, for adsorbate coverages below a ML.

The emersed (withdrawn) Cu(111) was then rinsed at OCP in water, to remove emersed electrolyte before its transfer to the analysis chamber. From Figure 3.4, oxygen was present on the surface at potentials above -0.7 V, though no Te was observed. Immersion of the Cu(111) into a basic solution at OCP results in the formation of a copper oxide/hydroxide layer [21, 22]. It appears that the peaks between -0.6 and -0.8 V correspond to reduction of the copper oxide/hydroxide layer to elemental Cu (Figure 3.3). That is, below -0.7 V the oxygen has been reduced away. In addition, Te was deposited, as evidenced by the increase in the Te/Cu AES ratio to more negative potentials. At -1.1 V the Te/Cu AES ratio maximizes, then drops at more negative potentials the Te/Cu AES ratio has a plateau at 0.75, at still more negative potentials. The drop was coincident with the reduction peak at -1.2 V (Figure 3.3), associated with bulk Te reduction to soluble telluride (Te^{2-}) [23-25].

The results in Figure 3.3 and 3.4 indicate that above -0.7 V the surface is oxidized before Te can deposit and that Te does not deposit on the oxide. From the Nernst equation, Ag/AgCl, pH 11 and 10^{-4} M HTeO_2^+ , the E^0 for Te formation should be around -0.6 V. Te deposition is known to be a kinetically slow process, and the oxide layer may further slow Te deposition till -0.7 V.

Figure 3.5 is a graph of O/Cu and Te/Cu AES ratios for the Cu(111) after 1 minute immersions in the acidic HTeO_2^+ solution, as a function of potential, to be contrasted with Figure 3.4 for the basic solution. No oxygen was observed on the Cu(111) substrate emersed from the pH 1 solution, at any potential, consistent with the

pourbaix diagram [26]. On the other hand, Te was present at all potentials studied. The Te/Cu ratio at -0.2 V (Figure 3.5) was 0.65, similar to the plateau value of 0.75 for the basic Te solution below -1.2 V (Figure 4). The Te/Cu ratio increased to 1.35 (Figure 3.5) at -0.6 V then drops to a plateau near 0.8 at potentials below -1.0 V, similarly to that observed in Figure 3.4. So for both the acidic and basic tellurite solutions, the Te/Cu AES ratios at the most negative potentials (Figure 3.4 and 3.5) were between 0.75 and 0.8.

LEED patterns observed for the Te deposits were $(\sqrt{3}\times\sqrt{3})R\ 30^\circ$ -Te (Figures 3.6A and 3.6B). Previous work by this group on Au(111) substrates also resulted in $(\sqrt{3}\times\sqrt{3})R\ 30^\circ$ patterns, produced by 1/3 ML hexagonal arrays of Te atoms, identified using both STM and UHV-EC with similar solutions and potentials[27, 28]. The previous Te on Au results showed that the last Te AL on the Au surface was more stable than bulk Te [29]. The Te/Cu AES ratio plateaus in Figures 3.4 and 3.5 suggest also increased stability for the last Te AL on the Cu(111) surface. It is proposed that immersion of the Cu(111) into either Te solution at negative potentials results in the formation of a 1/3 ML Te AL, with all other tellurite reduction resulting in soluble telluride ions.

Figure 3.7E is the Auger spectrum of a clean Cu(111) after confinement in the EC-ante-chamber with the electrochemical cell present and full of solution. The ante-chamber was back filled with an atmosphere of UHP Ar prior to insertion of the cell and solution vapor. It is proposed that this environment is similar to that encountered by a Cu wafer during transfer from one bath to the next at OCP inside a deposition tool. The

Cu(111) was held in the chamber for 5 minutes and resulted in an O/Cu AES ratio of 0.76 (Figure 3.7E).

The Cu(111) was then coated with a Te AL (Figure 3.7B) by electrodeposition from the basic TeO₂ solution at -1.32 V. The Auger spectrum showed the characteristic doublet for Te at 480 eV, and no signal for O at 503 eV. The Te modified Cu(111) was again exposed in the stainless steel EC-ante-chamber to atmospheric UHV Ar and solution vapor for 5 minutes (Figure 3.7C), resulting in no detectable oxygen AES signal. The tellurium modified Cu(111) was then exposed to ambient air for 12 minutes and transferred back to the main chamber for surface characterization (Figure 3.7D). A trace of oxygen, near the limit of detection, was evident, however, the results indicate that the Te AL effectively protected the Cu(111) surface from oxidation under ambient air conditions.

Selenium

Figure 3.8 shows Se/Cu and O/Cu AES ratios for the Cu(111) immersed into the pH 4.7 Se solution, as a function of potential. The Auger yield for Se is relatively low, making the Se AES signal difficult to measure at low coverage. The presence of oxygen and absence of Se at potentials positive of -0.7 indicate that a Se protective layer was not formed under those conditions. However, the absence of oxygen and presence of Se for potentials below -0.7 V indicates that Se has adsorbed and protects the surface from oxidation by passivating during emersion. Figure 3.6C is a ($\sqrt{3}\times\sqrt{3}$)R 30° LEED pattern for the Se layer, though with significant diffused intensity, indicating some disorder in Se modified surface.

After AES and LEED, the Se modified Cu(111) was transferred back to the UHV-EC ante-chamber, and exposed to 1 atm of UHP Ar and solution vapor for 5 minutes. The resulting AES spectrum of the Se modified Cu(111) revealed the presence of oxygen, resulting in a O/Cu AES ratio 0.06, to be compared with 0.8 in the absence of the Se (Figure 3.7E). Evidently, a Se AL was not as good at protecting from oxidation by passivating the Cu(111) as a Te AL, but was still effective. Exposure of the Se modified Cu(111) to 1 atm of oxygen, by purging industrial grade oxygen (99.99%) into the ante-chamber for 11 minutes, resulted in an O/Cu AES ratio of 1.2, indicating a failure to protect from oxidation by passivation.

Iodine

The adsorption of Cl, Br, and I have been studied on many metal surfaces [30]. For many metals, I atoms adsorb most strongly, relative to Br and Cl [31-33]. For example, iodine adsorption resulted in formation of both a $(\sqrt{3}\times\sqrt{3})R 30^\circ$ [34] and (3×3) [35] structures on Au(111) at higher and lower potentials respectively. In the present study, the Cu(111) was immersed in 10 mM KI solution at OCP, then scanned to -0.73V to prevent formation of multiple ML of CuI [2]. The Cu(111) was then emersed, rinsed with DI water and transferred to the analysis chamber for characterization. The Auger spectrum of the surface (Figure 3.9A) showed the characteristic doublet for iodine, while the LEED pattern (Figure 3.6D) was a clear $(\sqrt{3}\times\sqrt{3})R 30^\circ$, believed to result from 1/3 ML of I atoms on the Cu(111) surface.

Figure 3.9 shows a comparison of the AES spectra for the iodine modified Cu(111) as formed (A), after exposure to solution vapors in UHP Ar for 10 min (B), and

after 12 minutes in 1 atm of oxygen (C). The absence of an oxygen signal in the Auger spectra has been used in the Te and Se studies as an indication of protection of the Cu(111) from oxidation by passivation. However the AES signals for oxygen and iodine overlap, making quantification of the O AES signal difficult. The best indication of the absence of oxygen is the resolution of the iodine doublet at 510 eV. The doublet becomes less resolved the greater the oxygen signal. The doublet in Figure 3.9A is for iodine in the absence of oxygen. However, after exposure to the solution vapor, Figure 3.9B, the depth of the doublet has noticeably decreased due to a small amount of oxygen pick-up. After exposure to 1 atm of O₂, the doublet is still present, but the oxygen signal has a similar magnitude to that for iodine, indicating breakdown of the passivating I atom layer.

Conclusion

Te, Se, and I atomic layers were deposited on Cu(111) surfaces. Adsorbed layers of all three elements showed ($\sqrt{3}\times\sqrt{3}$) R 30⁰ unit cells, via LEED, pattern though the Se pattern displayed significant diffuse intensity, suggesting some disorder in the layer. Upon exposure to solution vapors in 1 atm of UHP Ar, no significant uptake of oxygen was measured, though small increases in oxygen were detected with the Se AL and the I AL (Table 1). Upon exposure to oxygen at atmospheric pressures for over 10 minutes, only the Te AL provided protection of the Cu(111), from oxidation by passivation while significant oxygen uptake was detected on both the Se and I treated surfaces (Table 1).

The success of the Te AL in preventing oxygen uptake on the Cu(111) recommends it as a possible atomic layer passivating agent. The next question was how to remove the layer prior to subsequent process steps. A range of electrochemical

treatments were investigated, as a function of the potential and pH, and none were successful in removing the layer. However, it has been shown that conformal deposits of a range of metals can be electrodeposited on an AL of Te.

State	Te (basic/acidic)	Se	I
As deposited	No oxygen	No oxygen	No oxygen
After exposure to solution vapors (10 minutes)	No oxygen	O/Cu = 0.06	O/Cu ~ 0.1
After exposure to ambient air (10 minutes)	No oxygen	O/Cu = 1.2	O/Cu ~ 0.4

Table 3.1. Comparison of AES peak to peak O/Cu ratios of modified Cu(111) surface before exposure and after exposure to solution vapors and ambient air.

Acknowledgements

Acknowledgments are made to Atotech for initial support of this work, and to the National Science Foundation, Division of Materials Research for subsequent support.

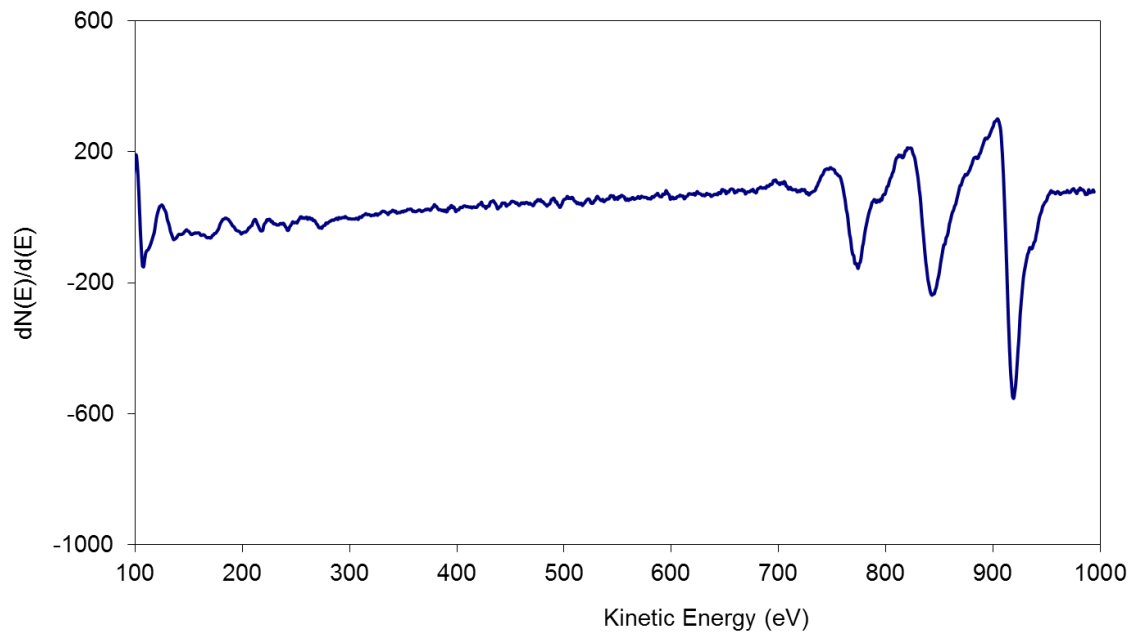


Figure 3.1. Clean Auger spectra of Cu(111)

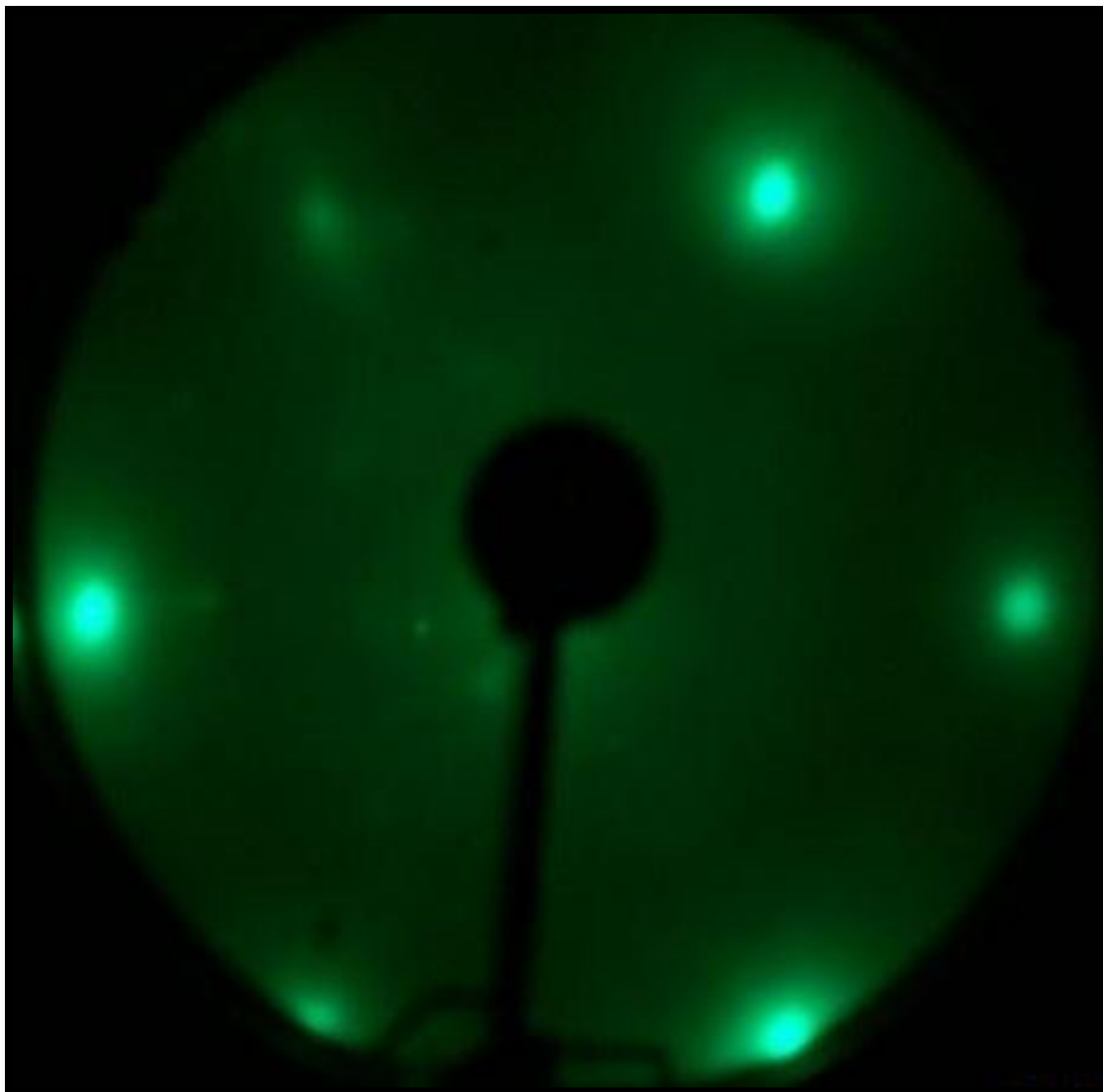


Figure 3.2. LEED pattern of Cu(111) at 60eV beam energy

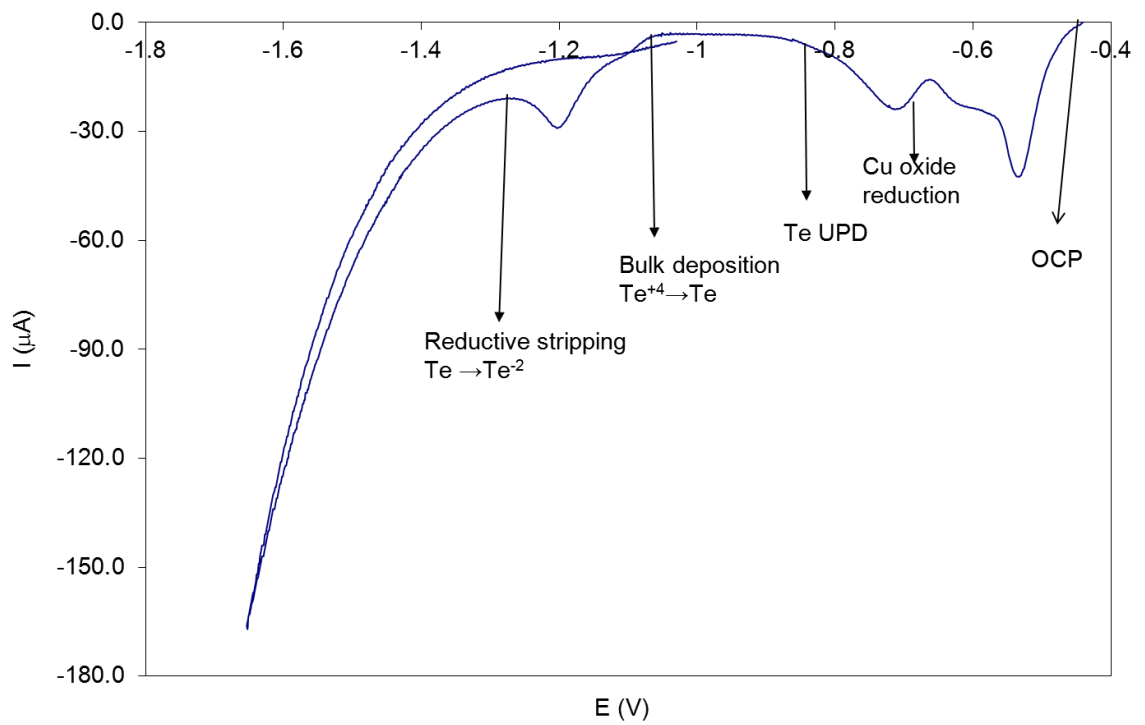


Figure 3.3. CV of Cu(111) in 0.1mM TeO₂ and 20mM NaOH solution at a scan rate of 5mV/s

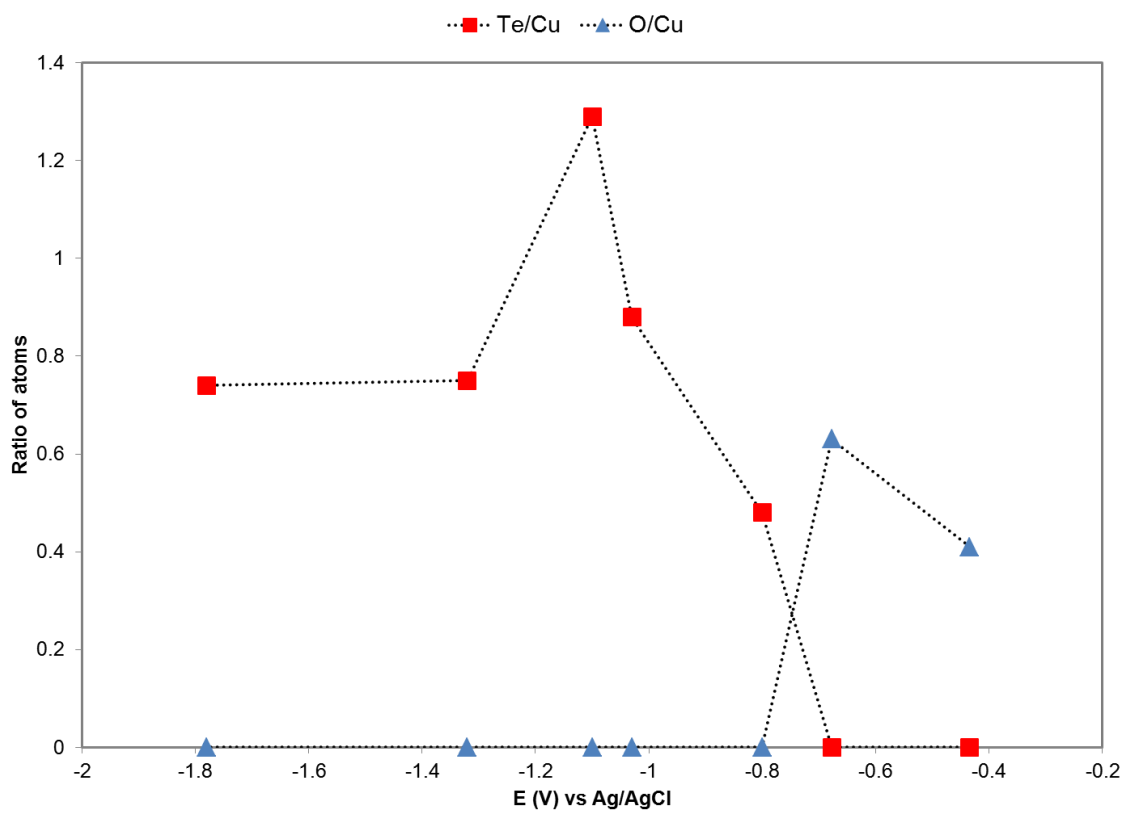


Figure 3.4. Auger ratio of Te/Cu and O/Cu at different deposition potentials of Te on Cu(111) from a basic solution of Te.

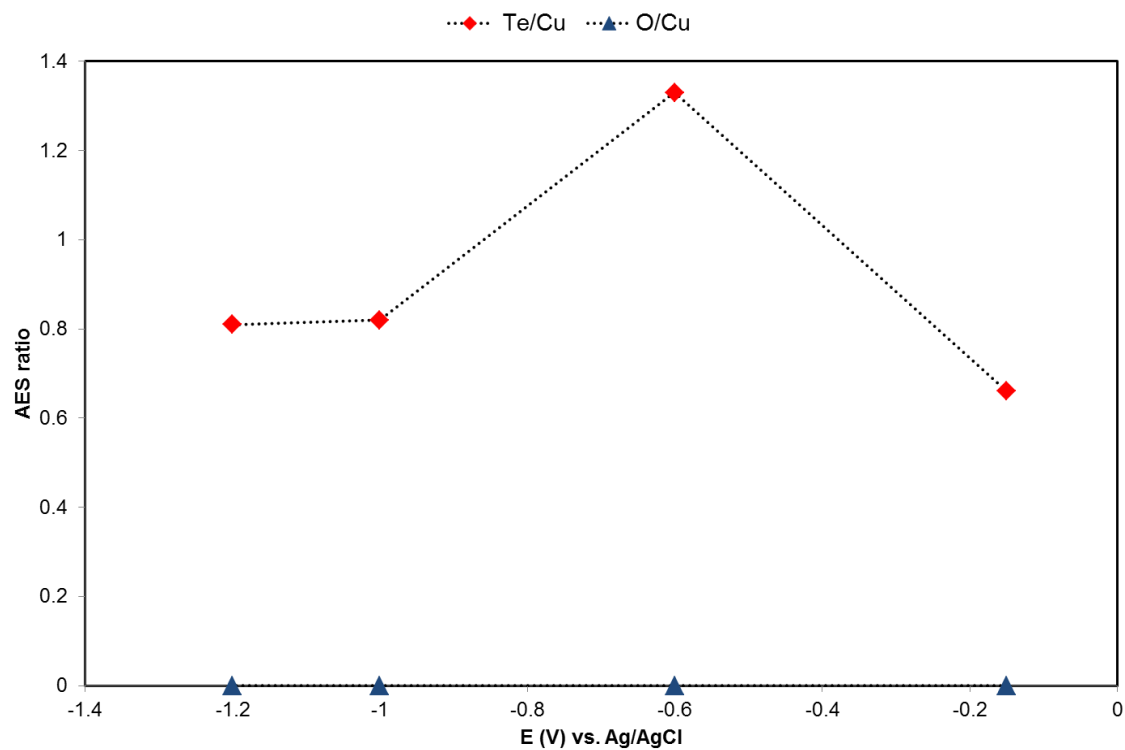


Figure 3.5. Auger ratio of Te/Cu and O/Cu at different deposition potentials of Te on Cu(111) from an acidic solution of Te.

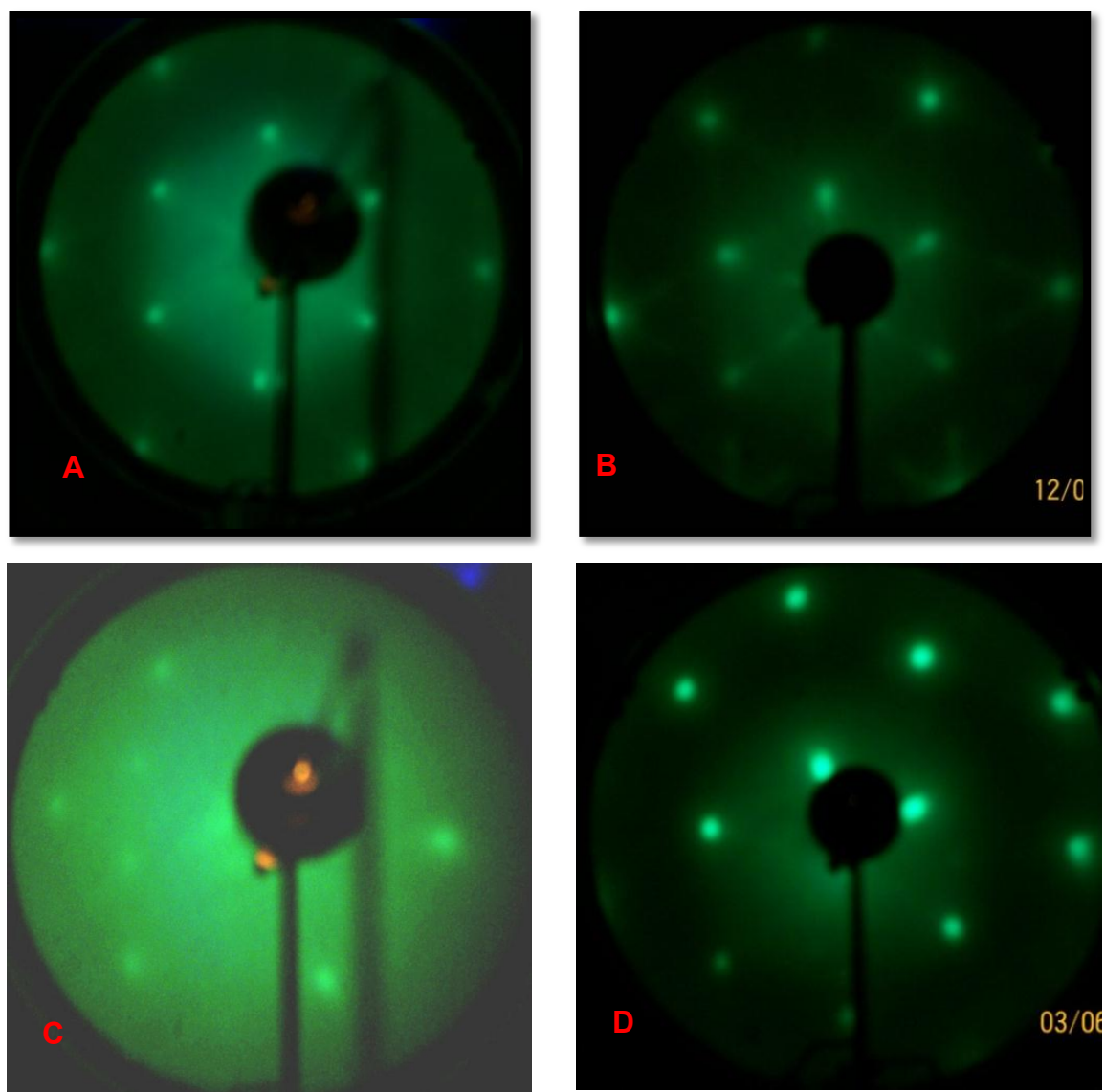


Figure 3.6. LEED patterns at 55eV beam energy of: (A) Te on Cu(111) from an acidic solution of Te at -1.0V, (B) Te on Cu(111) from a basic solution at -1.32V, (C) Se on Cu(111) at -0.73V, (D) I on Cu(111) at -0.73V

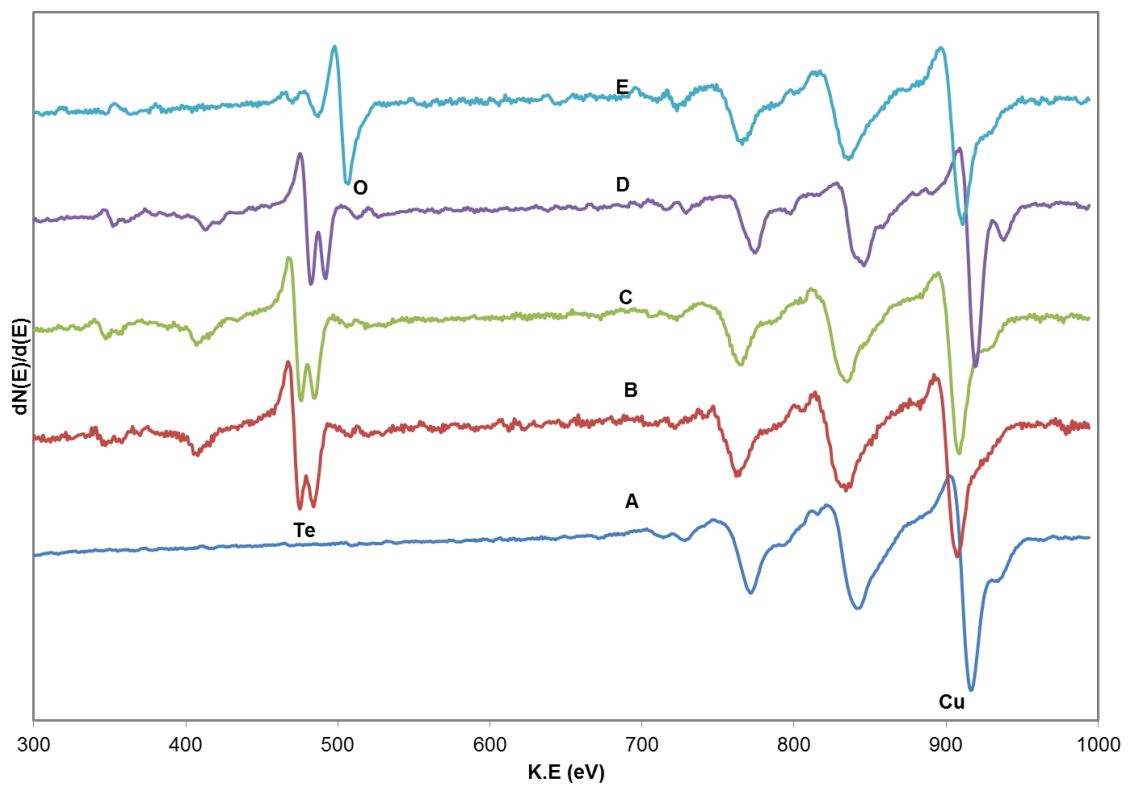


Figure 3.7. AES spectra of: (A) Clean Cu(111), (B) Cu(111) after the deposition of Te, (C) Te on Cu(111) after exposure to solution vapors, (D) Te on Cu(111) after exposure to ambient air and (E) Clean Cu(111) after exposure to solution vapors.

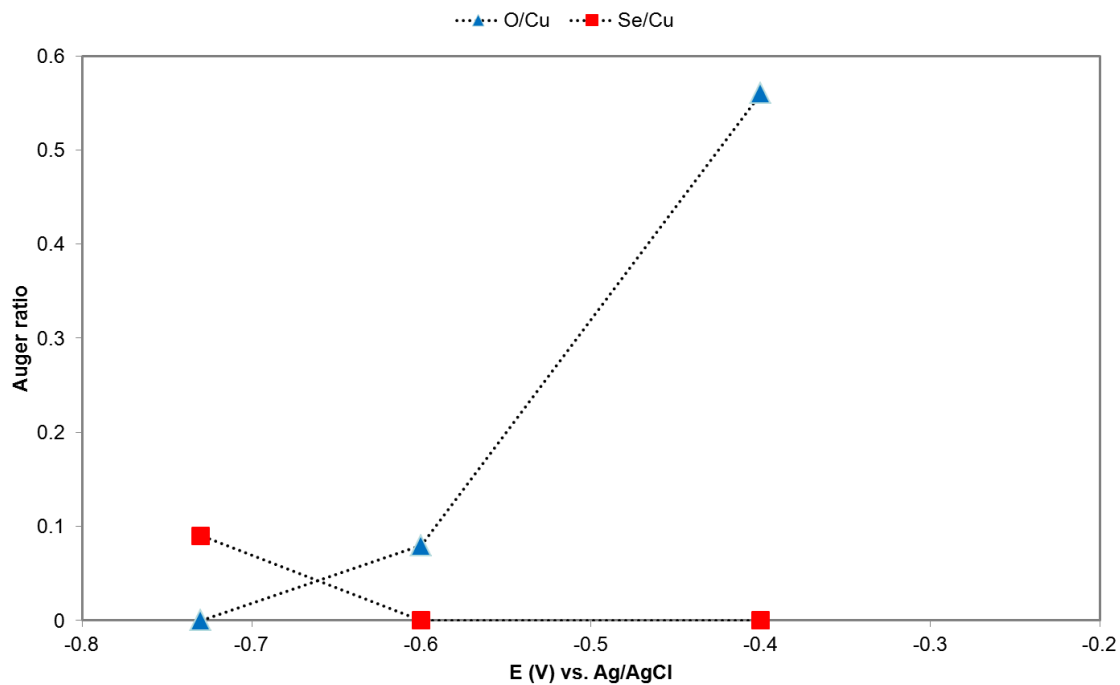


Figure 3.8. Auger ratio of elements after Se deposition on Cu(111) at different potentials in 0.1mM SeO₂ and 20mM NaClO₄ .

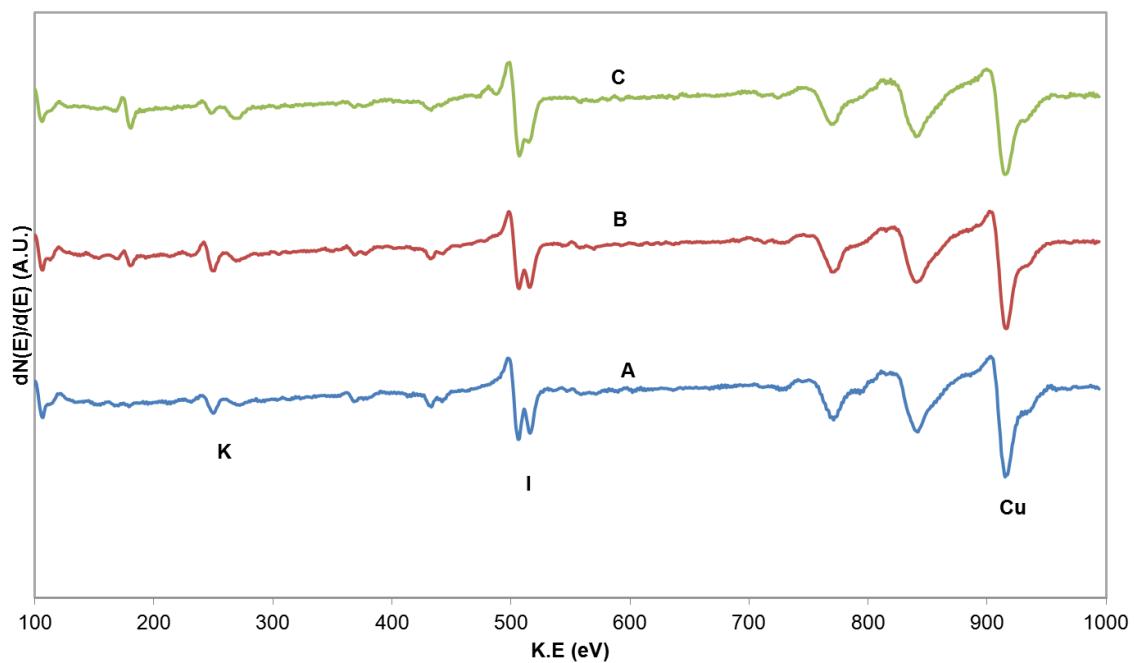


Figure 3.9. AES of: (A) Cu(111) after iodine deposition at -0.73V, (B) I on Cu(111) after exposure to solution vapors for 10 minutes, (C) I on Cu(111) after exposure to 1 atm of oxygen for 12 minutes.

References

1. Andricacos, P.C., *Copper on-chip interconnections*. Interface, 1999. **8**(1): p. 32.
2. Hai, N.T.M., et al., *Combined scanning tunneling microscopy and synchrotron X-ray photoemission spectroscopy results on the oxidative CuI film formation on Cu(111)*. Journal of Physical Chemistry C, 2007. **111**(40): p. 14768-14781.
3. Vereecken, P.M., et al., *The chemistry of additives in damascene copper plating*. Ibm Journal of Research and Development, 2005. **49**(1): p. 3-18.
4. Josell, D., D. Wheeler, and T.P. Moffat, *Gold Superfill in Submicrometer Trenches: Experiment and Prediction*. Journal of The Electrochemical Society, 2006. **153**(1): p. C11-C18.
5. Moffat, T.P., et al., *Superconformal film growth: Mechanism and quantification*. Ibm Journal of Research and Development, 2005. **49**(1): p. 19-36.
6. Andricacos, P.C., et al., *Damascene copper electroplating for chip interconnections*. IBM Journal of Research and Development, 1998. **42**(5): p. 567-574.
7. Kang, M.C., et al., *Local Corrosion of the Oxide Passivation Layer during Cu Chemical Mechanical Polishing*. Electrochemical and Solid State Letters, 2009. **12**(12): p. H433-H436.
8. Ehlers, C.B. and J.L. Stickney, *Surface chemistry of copper(100) in acidic sulfate solutions*. Surface Science, 1990. **239**(1-2): p. 85-102.
9. Kim, J.Y., Y.G. Kim, and J.L. Stickney, *Cu nanofilm formation by electrochemical atomic layer deposition (ALD) in the presence of chloride ions*. Journal of Electroanalytical Chemistry, 2008. **621**(2): p. 205-213.

10. Chia, V.K.F., et al., *Adsorption and orientation of hydroquinone and hydroquinone sulfonate at platinum electrodes. Studies by thin-layer electrochemistry, LEED, Auger and infrared spectroscopy.* Journal of Electroanalytical Chemistry and Interfacial Electrochemistry, 1984. **163**(1-2): p. 407-13.
11. Stickney, J.L., S.D. Rosasco, and A.T. Hubbard, *Electrodeposition of Copper on Pt(111) Surfaces Pretreated with Iodine. Studies by LEED, Auger Spectroscopy and Electrochemistry.* JECS, 1983. **131**: p. 260.
12. Liu, J., et al., *The effects of an iodine surface layer on Ru reactivity in air and during Cu electrodeposition.* Journal of The Electrochemical Society, 2005. **152**(2): p. G115-G121.
13. Kim, J.Y., Y.-G. Kim, and J.L. Stickney, *Cu nanofilm formation by electrochemical atomic layer deposition (ALD) in the presence of chloride ions.* J. Electroanal. Chem. FIELD Full Journal Title:Journal of Electroanalytical Chemistry, 2008. **621**(2): p. 205-213.
14. An, K.S., et al., *Epitaxial growth of Sb thin film and chemical reaction of Sb-induced surface reconstruction on Si(1 1 3)3×2.* Surface Science, 2001. **492**(1-2): p. L705-L710.
15. Kolb, D.M., *Physical and Electrochemical Properties of Metal Monolayers on Metallic Substrates,* in *Advances in Electrochemistry and Electrochemical Engineering*, H. Gerischer and C.W. Tobias, Editors. 1978, John Wiley: New York. p. 125.

16. Juttner, K. and W.J. Lorenz, *Underpotential Metal Deposition on Single Crystal Surfaces*. Z. Phys. Chem. N. F., 1980. **122**: p. 163.
17. Adzic, R.R., *Electrocatalytic Properties of the Surfaces Modified by Foreign Metal Ad Atoms*, in *Advances in Electrochemistry and Electrochemical Engineering*, H. Gerishcher and C.W. Tobias, Editors. 1984, Wiley-Interscience: New York. p. 159.
18. Gewirth, A.A. and B.K. Niece, *Electrochemical applications of in situ scanning probe microscopy*. Chem. Rev., 1997. **97**: p. 1129-1162.
19. Herrero, E., L.J. Buller, and H.D. Abruna, *Underpotential Deposition at Single Crystal Electrodes Surfaces of Au, Pt, Ag and other Materials*. Chemical Reviews, 2001. **101**: p. 1897-1930.
20. Magnussen, O.M., *Ordered anion adlayers on metal electrode surfaces*. Chemical Reviews, 2002. **102**(3): p. 679-725.
21. Harris, J.E., et al., *Reductive elimination of surface-coordinated iodine at platinum electrodes: the influence of codeposited silver*. Journal of Physical Chemistry, 1989. **93**(6): p. 2610-14.
22. Ehlers, C.B., I. Villegas, and J.L. Stickney, *The surface chemistry of Cu (100) in HCl solutions as a function of potential: a study by LEED, Auger spectroscopy and depth profiling*. Journal of Electroanalytical Chemistry, 1990. **284**(2): p. 403-412.
23. Forni, F., et al., *Electrochemical aspects of CdTe growth on the face (111) of silver by ECALE*. Electrochimica Acta, 2000. **45**(20): p. 3225-3231.

24. Saloniemi, H., et al., *Electrochemical quartz crystal microbalance and cyclic voltammetry studies on PbSe electrodeposition mechanisms*. Journal of Materials Chemistry, 2000. **10**(2): p. 519-525.
25. Sorenson, T.A., et al., *Formation of and phase transitions in electrodeposited tellurium atomic layers on Au(111)*. Surface Science, 2001. **470**(3): p. 197-214.
26. Kemell, M., et al., *One-step electrodeposition of Cu_{2-x}Se and CuInSe₂ thin films by the induced co-deposition mechanism*. Journal of the Electrochemical Society, 2000. **147**(3): p. 1080-1087.
27. Lay, M.D. and J.L. Stickney, *EC-STM Studies of Te and CdTe Atomic Layer Formation from a Basic Te Solution*. Journal of the Electrochemical Society, 2004. **151**(6): p. C431-C435.
28. Stickney, J.L., et al., *Compound semiconductor formation by electrochemical atomic layer epitaxy (EC-ALE): Surface Chemistry*, in *Encyclopedia of Surface and Colloid Science*, A.T. Hubbard, Editor. 2002, Marcel Dekker, Inc.: New York. p. 1129-1161.
29. Colletti, L.P., et al., *Thin layer electrochemical studies of ZnS, ZnSe, and ZnTe formation by electrochemical atomic layer epitaxy (ECALE)*. Materials Research Society Symposium Proceedings, 1997. **451**(Electrochemical Synthesis and Modification of Materials): p. 235-244.
30. Magnussen, O., *Electrochemistry of Nanomaterials. Edited by G. Hodes*. ChemPhysChem. Vol. 3. 2002. 130-131.

31. Martinez-Ruiz, A., M. Palomar-Pardave, and N. Batina, *Overpotential deposition of copper on an iodine-modified Au(111) electrode*. *Electrochimica Acta*, 2008. **53**(5): p. 2115-2120.
32. Harrington, D.A., et al., *Films formed on well-defined stainless steel single-crystal surfaces in oxygen and water: studies of the (111) plane by LEED, Auger, and XPS*. *Corrosion Science*, 1985. **25**(10): p. 849-69.
33. Ham, D., K.K. Mishra, and K. Rajeshwar, *Anodic Electrosynthesis of Cadmium Selenide Thin-Films - Characterization and Comparison with the Passive Transpassive Behavior of the Cds, Cdte Counterparts*. *Journal of the Electrochemical Society*, 1991. **138**(1): p. 100-108.
34. Bravo, B.G., et al., *Anodic underpotential deposition and cathodic stripping of iodine at polycrystalline and single-crystal gold. Studies by LEED, AES, XPS and electrochemistry*. *Journal of Physical Chemistry*, 1991. **95**: p. 5245.
35. Roux, H., N. Boutaoui, and M. Tholomier, *AES quantitative interpretation of the first stages of palladium silicide (Pd₂Si) formation during palladium adsorption on silicon(111) at room temperature*. *Surface Science*, 1992. **260**(1-3): p. 113-15.

CHAPTER 4
ELECTROCHEMICAL ULTRA HIGH VACUUM STUDIES OF GERMANIUM
ATOMIC LAYER FORMATION ON Au(111)³

³ Daniel K. Gebregziabher Nagarajan Jayaraju Youn-Geun Kim, Xuehai Liang and John L. Stickney
University of Georgia, Athens, GA, 30602, To be submitted to ECS.

Abstract

Germanium was deposited on a clean Au(111) single crystal from a 0.1 mM aqueous solution of GeO_2 and 2 mM K_2SO_4 solution. Different deposition potentials ranging from -0.765 V to -1.4 V were investigated. In order to understand the electrochemical processes taking place during these studies, analytical tools like cyclic voltammogram (CV), Auger electron spectroscopy (AES), electrochemical quartz microbalance (EQCM) and scanning tunneling microscopy (STM) were used. Surface analysis of the deposits using AES showed that the Ge/Au peak to peak Auger ratio increased as more negative potentials were investigated but no clear LEED patterns were observed in this potential range which were used for the deposition of Ge. This may be the result of oxidation of the Ge upon emersion of the electrode from the solution. *In-situ* STM studies showed that Ge forms a $(\sqrt{3}\times\sqrt{3})$ -Ge structure at -0.45 V and both $(\sqrt{3}\times\sqrt{3})$ -Ge and distorted (3x3)-Ge structure at -0.60 V. It appears that Ge formed a layer of hydroxide around -0.70 V and this was confirmed by the presence of an oxygen signal in the AES. EQCM data showed that there was a significant mass increase between -0.2 V and -0.7 V which further confirms that the Ge was oxidized since there was no significant increase in the Auger signal of the Ge. There was a significant decrease in the oxygen Auger signal at -1.3 V, and this could be the result of a germanium hydride formation before the onset of hydrogen evolution at more negative potentials.

Introduction

Si has almost a perfect interface with its thermally grown oxide which acts as an effective mask in device manufacturing. It has also an extremely low surface state density at the Si/SiO₂ interface. These properties makes it important in the electronics industry [1]. But further scaling down of Si/SiO₂ based transistors is at an end for future high performance devices.

Germanium is of interest because it has high hole (1900 vs. 500cm²/V-s) and electron (3900 vs. 1400cm²/V-s) mobility as compared to silicon [2, 3]. In Si based devices, germanium has possible applications as a photo-detector and high mobility channel field effect transistors and it can also be used as a substrate for growing III-V compound semiconductors in multi-junction photovoltaic cells [4, 5]. Some limitations to using Germanium is that it has higher density of states as compared to silicon, it has a narrower band gap and its thermally grown oxide is not as perfect and as good a dielectric as silicon dioxide [1]. Germanium is also very expensive when compared to silicon (\$3900 vs. \$54/kg) [6]. The deposition of high-*k* dielectric materials such as HfO₂, Al₂O₃, and ZrO₂ on germanium substrate have been reported [7] and these materials could be used to replace the not so perfect GeO₂.

The electrodeposition of germanium has mainly been achieved from ionic solutions due to its low over potential for hydrogen evolution in aqueous solutions [8, 9]. Epitaxial growth of germanium can also be achieved by molecular beam epitaxy (MBE) and ultrahigh vacuum chemical vapor deposition (UHV-CVD) [4].

The purpose of this study was to investigate electrodeposition of germanium on Au(111) single crystal from aqueous solutions and study the interaction between the first

layer of germanium and the gold single crystal. If the first atomic layer can be deposited and its growth controlled, then this phenomena can be used for growing atomic layers of germanium which can be used for optoelectronic materials.

Experimental

Reagent quality K_2SO_4 (J.T. Baker), GeO_2 (Johnson Matthey) and Barnstead Nanopure 18 M Ω -cm water were used to prepare the solutions. The electrochemistry was carried out in an electrochemical cell with three electrode configuration inside a UHV compatible stainless steel ante-chamber in which Au(111) single crystal disc was the working electrode, Au wire was the auxiliary electrode and Ag/AgCl (3 M KCl) (Bio Analytical Systems) was the reference electrode. A μ Autolab Type III Potentiostat/Galvanostat (Eco Chemie B.V.) was used to control the potentials. The solutions were degassed with high purity Ar (99.998%) for one hour prior to electrochemical studies. The ante-chamber was back filled to atmospheric pressure with high purity Ar-gas (99.998%) while the electrochemical experiments were performed. After the electrochemical reactions were performed the cell was removed from the ante-chamber through a 4.5" gate valve and the ante-chamber was pumped down so the sample could be transferred to the main analysis chamber for characterization, without exposure to air. All potentials in this study were reported versus Ag/AgCl (3 M KCl) reference electrode.

The analysis chamber was equipped with optics for LEED (Princeton Research Instruments, Inc.) and a cylindrical mirror analyzer for AES (Perkin-Elmer). STM studies were performed in solution, using a Nanoscope 3 (Veeco). EQCM studies were

performed using gold working, gold wire auxiliary and Ag/AgCl (3 M KCl) reference electrodes.

The Au (111) single crystal electrode was cleaned by ion bombardment and annealed in a UHV chamber prior to any electrochemical reactions. LEED pattern of the cleaned Au(111) showed a clear (1x1) pattern (Figure 4.1), indicating a well ordered surface. Figure 4.2 shows the Auger spectra of clean Au(111) after cold Ar⁺ ion bombardment and annealing. Germanium was then deposited on the Au (111) single crystal electrode from an aqueous solution of GeO₂ in 2mM K₂SO₄ solution, at different potentials between -0.765V and -1.4V.

Results and Discussion

Figure 4.3 shows a cyclic voltammetry of Au(111) single crystal in 0.1 mM GeO₂ and 2 mM K₂SO₄ solution with a pH of 4.5 at a scan rate of 5 mV/s. The clean Au(111) single crystal was immersed in the solution at open circuit potential (0.173 V). Initially the potential was scanned in the negative direction to -1.4 V and then was reversed and scanned in the positive direction to 0.4 V. Several reductive and oxidative features were observed both during the negative and positive scan of the potential.

The reductive feature at ~ -0.800 V could be associated with the deposition of the first layer of Ge on Au(111). The Auger spectrum of this deposit shows the presence of Ge and oxygen (Figure 4.4) and this might be due to the formation of an oxide of the Ge at this potential. This is in agreement with the work of Maroun et. al. [10, 11] on reversibility of GeH/GeOH and hydrogen adsorption/desorption at germanium electrodes. The feature around -1.300 V could be associated with the reduction of the germanium oxide layer or the formation of a germanium hydride layer. Gerischer et. al. also

suggested that germanium hydroxide slowly converts to the hydride form during cathodic polarization [12] which was confirmed by the work of Kepler et. al [13]. Scanning the potential beyond -1.400 V in the negative direction resulted in hydrogen evolution reaction. The features in the positive going scan were the results of anodic dissolution of the germanium.

Based on the CV from Figure 4.3, the potential was stepped to different deposition potentials and was held at that potential for 180 s and the deposits were characterized by AES. Figure 4.4 shows the AES spectra of the deposits at different deposition potentials. As can be seen from the AES, the germanium signal increased whereas the oxygen signal decreased as more negative deposition potentials were investigated. No clear LEED patterns were observed in the potential range used for the deposition of germanium (Figure 4.1B). This may be the result of oxidation of the electrode upon emersion from the solution.

EQCM mass change measurements (Figure 4.5) were taken while recording the CV of gold in 1mM GeO_2 and 0.5M Na_2SO_4 , at a scan rate of 5mV/s. There was a significant mass increase between -0.2V and -0.7V but the fact that there was no significant Ge/Au AES ratio increase (Figure 4.4) support that a germanium oxide/hydroxide was formed in this potential range. The EQCM measurements did not show significant mass change between -0.7V and -1.0V and this could be attributed to the change in oxidation state of germanium from +4 to +2. In scanning the potential negative of -1.0 V there was significant change in the mass of the EQCM. The oxygen AES signal decreased while the Ge AES signal increased and this could be due to increased Ge deposition at more negative potentials. In the positive going scan no significant mass

change was observed before -0.2V during oxidative stripping and this could be an indication that only change in the oxidation state of germanium was taking place.

In-Situ STM studies were performed to understand the deposition process of Ge on Au(111) single crystal. The *In-Situ* STM image taken at -0.45 V (Figure 4.6A) showed a $(\sqrt{3}\times\sqrt{3})$ -Ge R30⁰ structure with a 1/3 monolayer (ML) coverage and when the potential was scanned towards more negative potentials a mixture of both (Figure 4.6B and 4.6C) $(\sqrt{3}\times\sqrt{3})$ -Ge R30⁰ and (3x3)-Ge R30⁰ were observed at -0.60 V indicating an increase in the coverage. At -0.80 V a Moiré pattern with coverage of 0.8 ML was observed (not shown here). The surface formed at this potential was atomically flat over a large surface [14] of about 300 nm.

Figure 4.7 shows the AES peak to peak ratio of atoms at different deposition potentials. The amount of germanium increased as more negative potentials were investigated. The presence of an oxygen signal agreed with the idea of the state of germanium as the oxide/hydroxide on the surface. At about -1.30 V there was a sudden decrease in the AES signal of oxygen and this was ascribed to the formation of a surface germanium hydride. There was a small increment in the germanium signal at -1.40 V but scanning in the negative direction beyond -1.40 V there was only hydrogen evolution reaction as was evident from the CV of Au(111) in germanium solution (Figure 4.3).

In order to quantify the amount of germanium deposited anodic stripping of the deposits was performed by holding the potential at 0.40 V for 60 s and as can be seen from Figure 4.8 the germanium coverage increased as the deposition potentials investigated became more negative. These coverages were plotted against the peak to peak ratio of Ge/Au and there was a linear relationship. The time for deposition at -1.40V

was varied and the observation was that after 180 s the amount of germanium deposited did not increase and this was confirmed by the charges from anodic stripping of the deposits. This was an indication that germanium electrodeposition from the aqueous solutions was self-limiting.

Conclusion

Germanium was deposited on Au(111) from an aqueous solution of 0.1mM GeO_2 in 2mM K_2SO_4 . The deposits were analyzed by Auger spectroscopy. From the Auger spectra it can be seen that the amount of germanium deposited increased as more negative potentials were investigated. The deposition was self-limiting because no increase was observed in the amount of Ge deposited negative of -1.40 V or increasing the deposition time at -1.4 V. *In-situ* STM measurements showed that a $(\sqrt{3}\times\sqrt{3})\text{-Ge R}30^\circ$ structure was formed at ~ -0.45 V with 1/3 ML coverage and a mixture of both $(\sqrt{3}\times\sqrt{3})\text{-Ge}$ and distorted $(3\times 3)\text{-Ge R}30^\circ$ structures at lower potentials. EQCM data showed that there was a significant mass increase between -0.2 V and -0.7 V and the presence of oxygen in the Auger spectra at these potentials was indicative that germanium exists in the form of an oxide/hydroxide. There was a significant decrease in the oxygen Auger signal at -1.3V and this was the result of formation of a germanium hydride, before the onset of hydrogen evolution, at more negative potentials.

Acknowledgments

Support of this work was from the National Science Foundation, DMR, which is gratefully acknowledged.

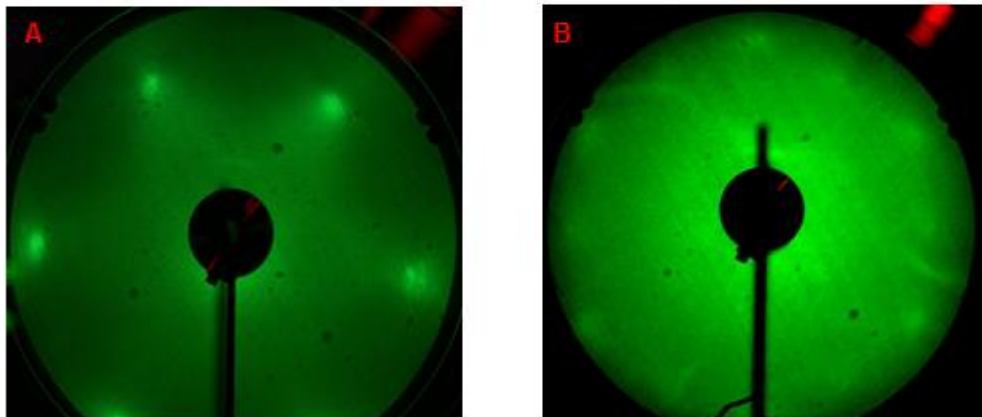


Figure 4.1. LEED pattern of Au (111) after cold Ar^+ ion bombardment and annealing (A) and Au(111) after Ge deposition at -1.4 V (B) in 0.1 mM GeO_2 solution at a beam energy of 50 eV.

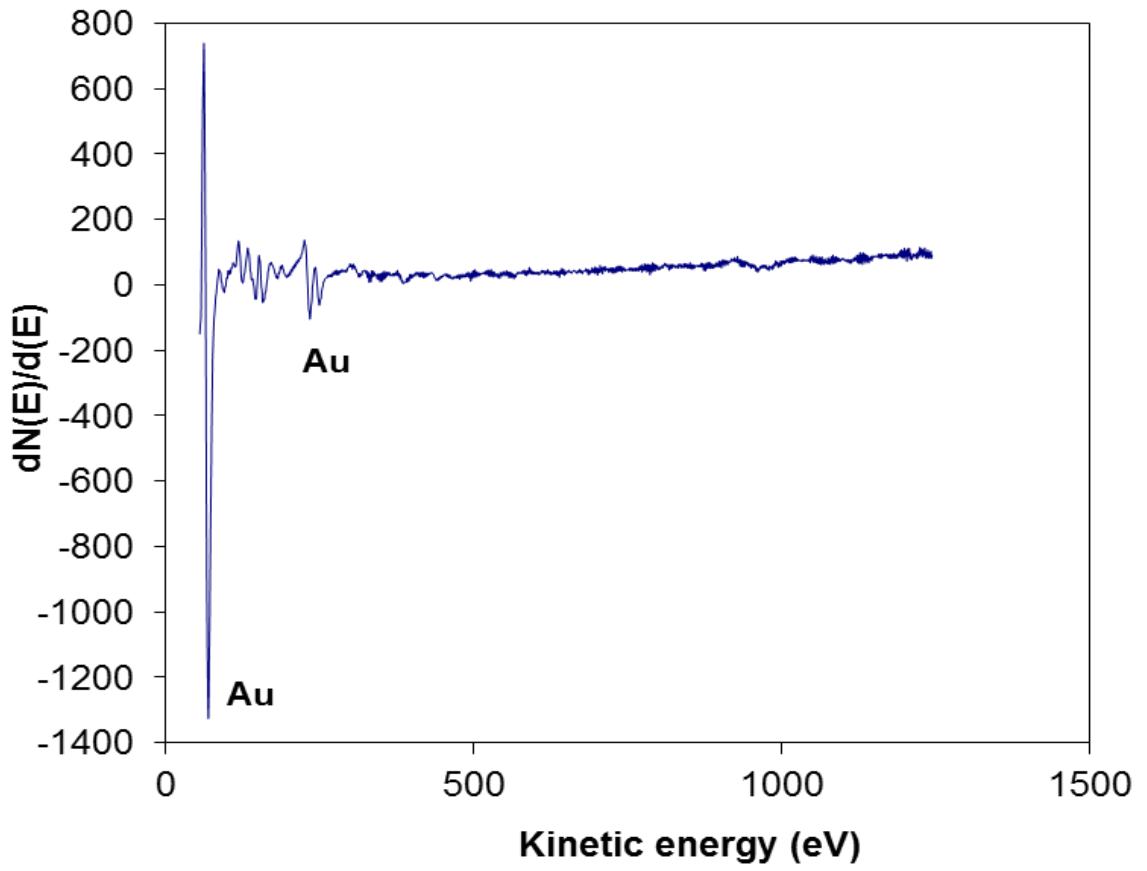


Figure 4.2. Auger spectra of a clean Au(111) after cold Ar^+ ion bombardment and annealing of the single crystal.

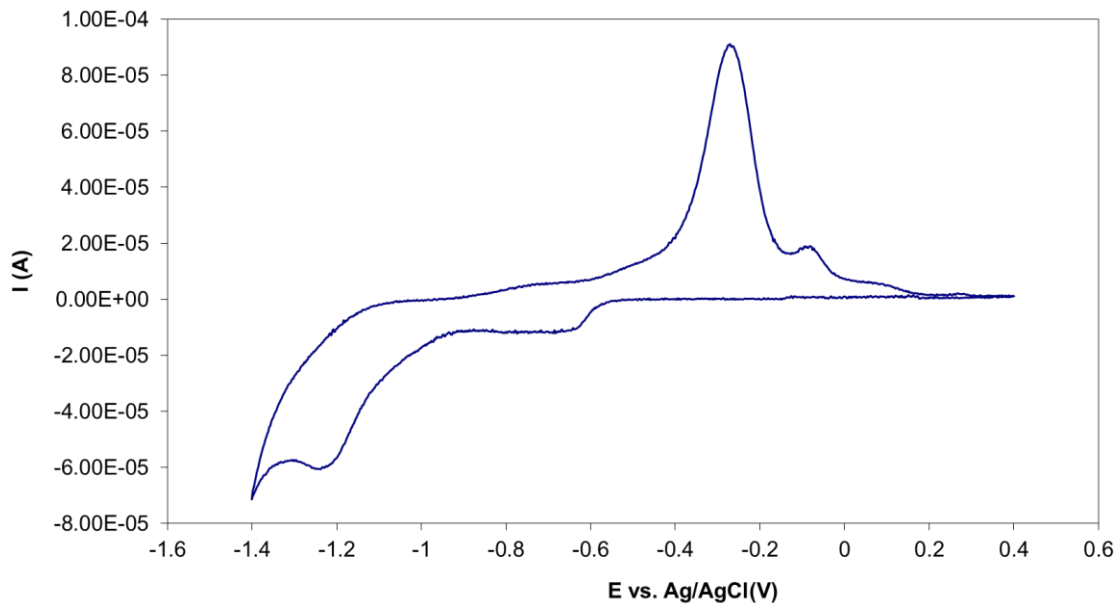


Figure 4.3. CV of Au(111) in 0.1 mM GeO_2 and 2 mM K_2SO_4 solution with a pH of 4.7 at a scan rate of 5 mV/s. The OCP was 0.173 V.

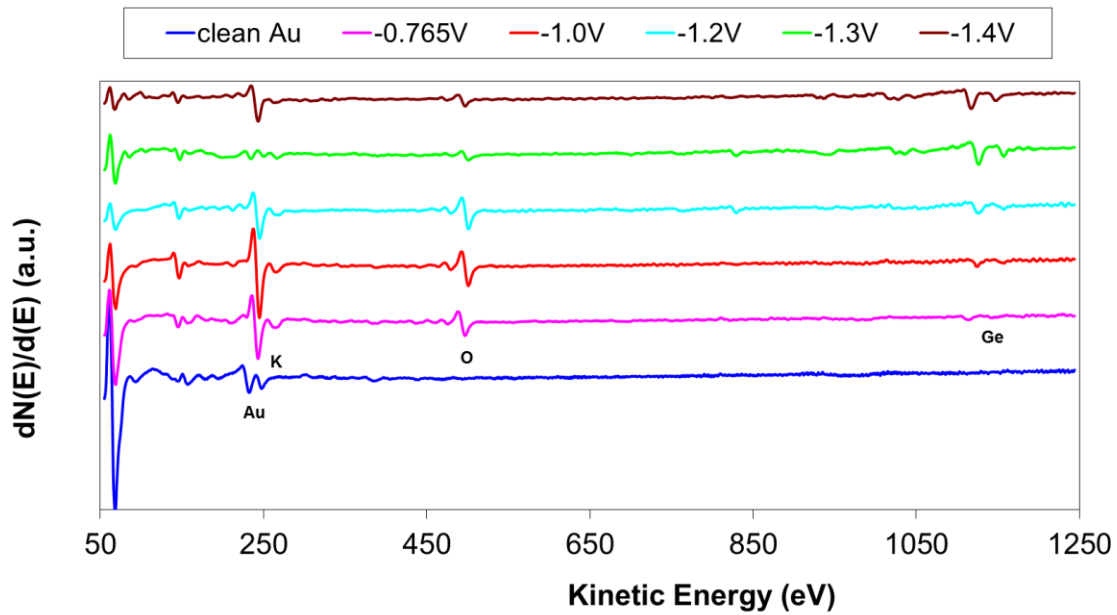


Figure 4.4. AES spectra of Ge deposited on Au (111) from a 0.1 mM Ge solution, pH 4.7, at different potentials.

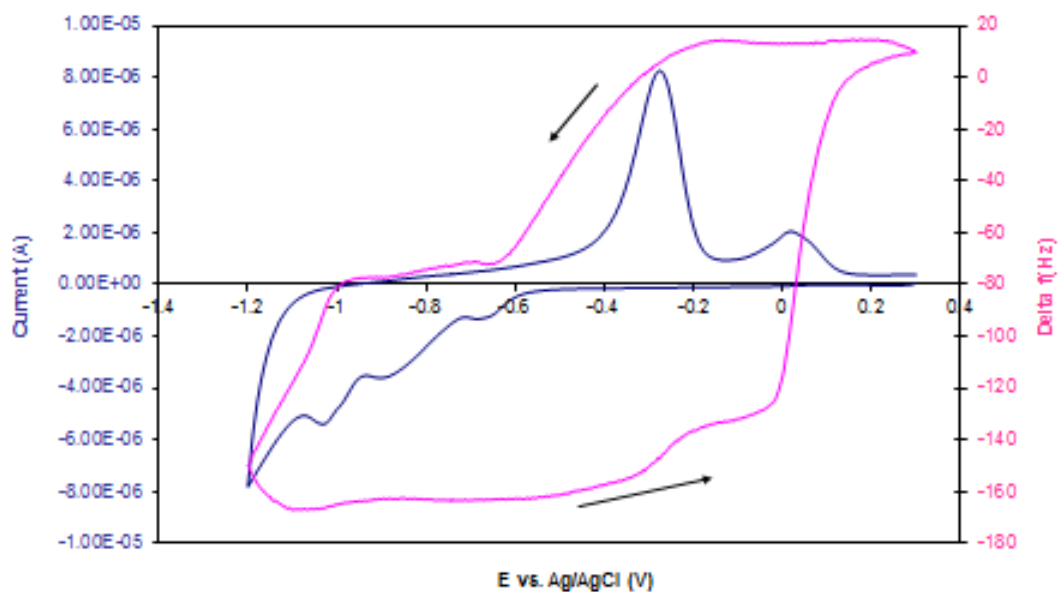


Figure 4.5. Simultaneous EQCM mass change measurements taken while recording the CV of Au(111) in 1mM GeO₂ and 0.5M Na₂SO₄ at a scan rate of 5 mV/s.

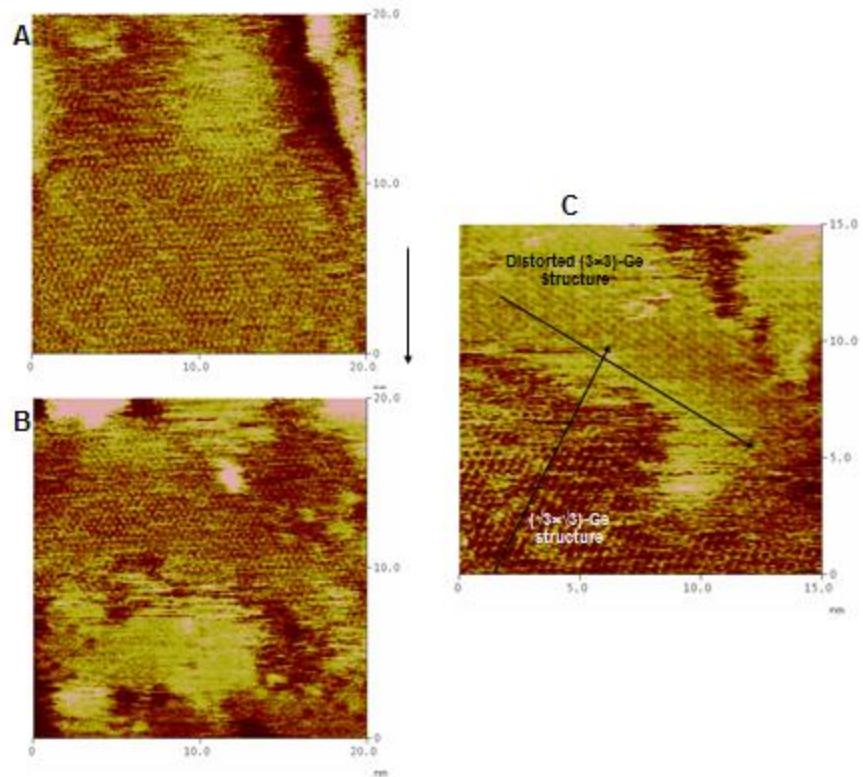


Figure 4.6. In-situ STM images of Ge on Au(111) at -0.450 V vs. Ag/AgCl exhibiting a $(\sqrt{3} \times \sqrt{3})$ -Ge structure (A) and at -0.600 V vs. Ag/AgCl exhibiting both $(\sqrt{3} \times \sqrt{3})$ -Ge and distorted (3×3) -Ge structure (B and C).

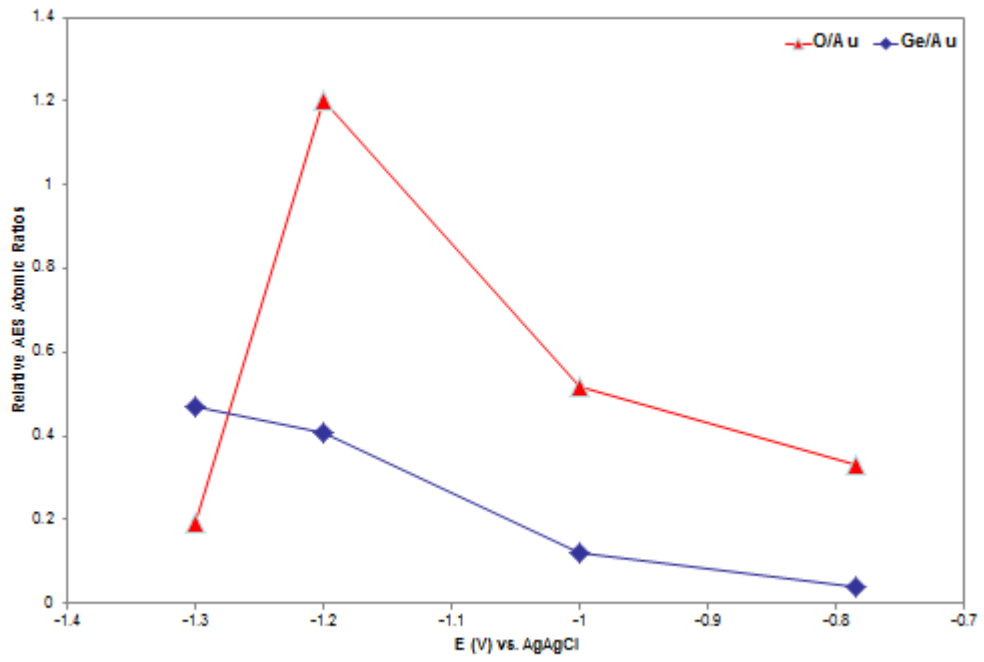


Figure 4.7. Relative AES peak to peak ratio of O/Au (triangles) and Ge/Au (diamonds) atoms at different potentials.

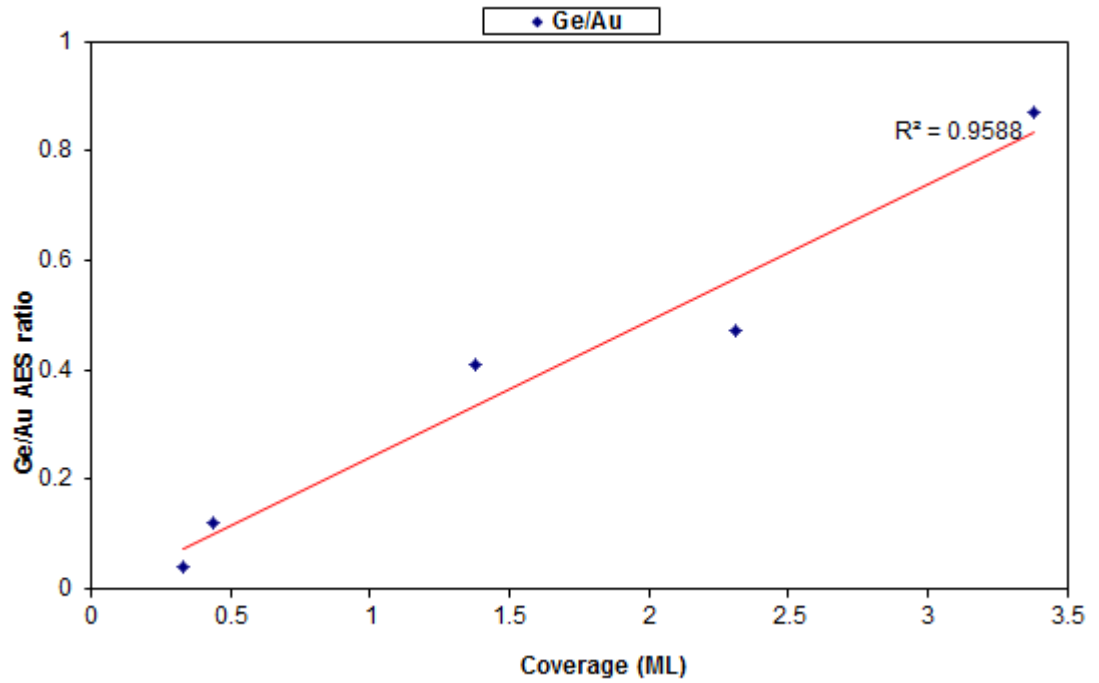


Figure 4.8. Plot of Ge coverages as a function of the relative AES peak to peak ratio of Ge/Au.

References

1. Haller, E.E., *Germanium: From its discovery to SiGe devices*. Materials Science in Semiconductor Processing, 2006. **9**(4-5): p. 408-422.
2. Rivillon, S., R.T. Brewer, and Y.J. Chabal, *Water reaction with chlorine-terminated silicon (111) and (100) surfaces*. Applied Physics Letters, 2005. **87**(17).
3. C. O. Chui, H.K., D. Chi, B. B. Triplett, P. C. McIntyre and K. C. Saraswat, IEDM 2002 Tech. Dig., 2002: p. 437.
4. Nylandsted Larsen, A., *Epitaxial growth of Ge and SiGe on Si substrates*. Materials Science in Semiconductor Processing, 2006. **9**(4-5): p. 454-459.
5. Van Elshocht, S., et al., *Study of CVD high-k gate oxides on high-mobility Ge and Ge/Si substrates*. Thin Solid Films, 2006. **508**(1-2): p. 1-5.
6. Brunco, D.P., et al., *Germanium: The Past and Possibly a Future Material for Microelectronics*. ECS Transactions, 2007. **11**(4): p. 479-493.
7. Bellenger, F., et al., *Electrical Passivation of the (100)Ge Surface by Its Thermal Oxide*. ECS Transactions, 2007. **11**(4): p. 451-459.
8. Endres, F. and S. Zein El Abedin, *Nanoscale electrodeposition of germanium on Au(111) from an ionic liquid: an in situ STM study of phase formation. Part I. Ge from GeBr₄*. Physical Chemistry Chemical Physics, 2002. **4**(9): p. 1640-1648.
9. Lokhande, C.D. and S.H. Pawar, *ELECTRODEPOSITION OF THIN-FILM SEMICONDUCTORS*. Physica Status Solidi a-Applied Research, 1989. **111**(1): p. 17-40.

10. Maroun, F., et al., *Reversibility of the GeH/GeOH transformation at a Ge electrode: an EQCM study*. Journal of Electroanalytical Chemistry, 2003. **549**: p. 161-163.
11. Maroun, F., F. Ozanam, and J.N. Chazalviel, *In-situ infrared monitoring of surface chemistry and free-carrier concentration correlated with voltammetry: Germanium, a model electrode*. Journal Of Physical Chemistry B, 1999. **103**(25): p. 5280-5288.
12. Gerischer, H., A. Mauerer, and W. Mindt, *Nachweis einer intermediären radikalstruktur der germanium-oberfläche beim Übergang zwischen hydrid- und hydroxidbelegung*. Surface Science, 1966. **4**(4): p. 431-439.
13. Kepler, K.D. and A.A. Gewirth, *In situ AFM and STM investigation of electrochemical hydride growth on Ge(110) and Ge(111) surfaces*. Surface Science, 1994. **303**(1-2): p. 101-13.
14. Liang, X.H., et al., *Aqueous Electrodeposition of Ge Monolayers*. Langmuir, 2010. **26**(4): p. 2877-2884.

CHAPTER 5

CONCLUSION

The main topic of this dissertation is UHV-EC studies of metal and semiconductor deposition. In Chapter 2 the growth of Cu nanofilms on e-beam sputtered 10nm Ru on Si(100) by electrochemical ALD was investigated. Since UPD of an element on itself is not possible, Pb was chosen as the sacrificial element to be exchanged for Cu in a process known as surface limited redox replacement reaction (galvanic displacement). Pb UPD was deposited onto a Cu UPD (UPD layer on Ru) and when a Cu^{2+} solution was flashed in at OCP the Pb UPD was replaced with Cu. This constituted one cycle. A linear dependence for Cu growth over 8 ALD cycles was shown and STM images showed a conformal deposit, as expected for an ALD process. Auger electron spectroscopy was used to show the relative Cu coverages and the charges for copper deposition were determined by using coulometry during oxidative stripping of the deposits. Using Cl^- containing electrolyte resulted in the adsorption of an atomic layer of Cl atoms, which have been shown to protect the surfaced from oxidation and this proved to be helpful at various stages of the deposition process.

Copper is a relatively reactive metal and it is susceptible to oxidation or contamination in ambient air. In Chapter 3 studies were carried out to investigate the passivation of Cu surface by depositing atomic layers of different elements. Te, Se, and I atomic layers were among the elements deposited on Cu(111) in an attempt to passivate the surface. Adsorbed layers of all three elements showed $(\sqrt{3}\times\sqrt{3}) R 30^0$ unit cells LEED

patterns although the Se LEED pattern displayed significantly diffuse intensity, suggesting some disorder in the layer. Upon exposure to solution vapors in 1 atm of UHP Ar, no significant uptake of oxygen was measured although small increases in oxygen were detected with the Se AL and the I AL. Upon exposure to oxygen at atmospheric pressures for over 10 minutes only the Te AL provided protection of the Cu(111) from oxidation while significant oxygen uptake was detected on both the Se and I treated surfaces.

The success of the Te AL in preventing oxygen uptake on the Cu(111) recommends it as a possible passivating agent. A range of electrochemical treatments were investigated, as a function of the potential and pH to remove the AL Te but none were successful in removing the layer. However, it has been shown that conformal deposits of a range of metals can be electrodeposited on an AL of Te.

Chapter 4 investigates the electrochemical deposition of Ge from an aqueous solution. Germanium was deposited on Au(111) from an aqueous solution of 0.1mM GeO_2 in 2mM K_2SO_4 . The deposits were analyzed by Auger spectroscopy. From the Auger spectra it can be seen that the amount of germanium deposited increased as more negative potentials were investigated. The deposition was self-limiting because no increase was observed beyond -1.40 V deposition potential. In-situ STM measurements showed that a $(\sqrt{3}\times\sqrt{3})$ -Ge $\text{R}30^\circ$ structure was formed at ~ -0.45 V with 1/3 ML coverage and a mixture of both $(\sqrt{3}\times\sqrt{3})$ -Ge and distorted (3×3) -Ge $\text{R}30^\circ$ structures at lower potentials. EQCM data showed that there was a significant mass increase between -0.2 V and -0.7 V and the presence of oxygen in the Auger spectra at these potentials was indicative that germanium exists in the form of a hydroxide. There was a significant

decrease in the oxygen Auger signal at -1.3V and this was the result of formation of a germanium hydride, before the onset of hydrogen evolution, at more negative potentials.

The metallization of back end of integrated circuits involves the deposition of seed layer of Cu on the barrier layer. This deposition is carried out by PVD but getting a conformal layer is very difficult especially if high aspect ratio vias and trenches are involved. EC-ALD can be a cheap alternative to PVD with the added advantage of conformal deposits in the vias and trenches. This might solve the issues associated with electrical resistance due to differences in the thickness of the seed layer formed by PVD at the top and bottom of the vias and trenches in damascene process. Therefore developing a cycle for the deposition of a seed layer of copper on barrier materials which are not good electrical conductors such as TiN/Ti and TaN is a good future prospect.